

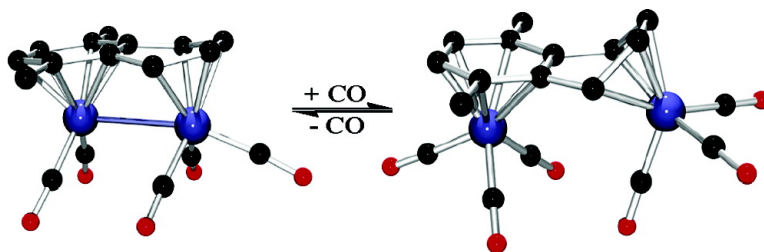
Article

Chemical and Electrochemical Reduction of Polyarene Manganese Tricarbonyl Cations: Hapticity Changes and Generation of *Syn*- and *Anti*-Facial Bimetallic η^5, η^5 -Naphthalene Complexes

Jeffrey A. Reingold, Kurtis L. Virkaitis, Gene B. Carpenter, Shouheng Sun, Dwight A. Sweigart, Paul T. Czech, and Kenneth R. Overly

J. Am. Chem. Soc., **2005**, 127 (31), 11146-11158 • DOI: 10.1021/ja0527370 • Publication Date (Web): 19 July 2005

Downloaded from <http://pubs.acs.org> on March 25, 2009



More About This Article

Additional resources and features associated with this article are available within the HTML version:

- Supporting Information
- Links to the 5 articles that cite this article, as of the time of this article download
- Access to high resolution figures
- Links to articles and content related to this article
- Copyright permission to reproduce figures and/or text from this article

[View the Full Text HTML](#)



ACS Publications
 High quality. High impact.

Chemical and Electrochemical Reduction of Polyarene Manganese Tricarbonyl Cations: Hapticity Changes and Generation of *Syn*- and *Anti*-Facial Bimetallic η^4, η^6 -Naphthalene Complexes

Jeffrey A. Reingold,[†] Kurtis L. Virkaitis,[†] Gene B. Carpenter,[†] Shouheng Sun,[†] Dwight A. Sweigart,^{†,*} Paul T. Czech,[‡] and Kenneth R. Overly[‡]

Contribution from the Departments of Chemistry, Brown University, Providence, Rhode Island 02912, and Providence College, Providence, Rhode Island 02918

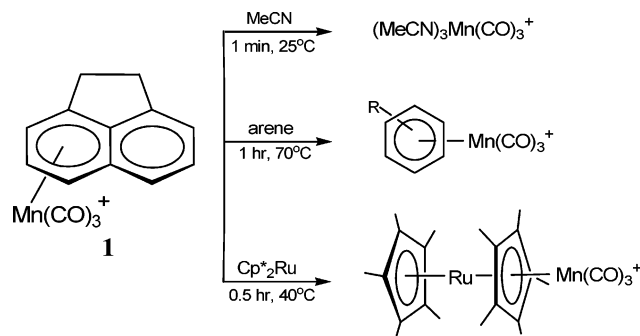
Received April 27, 2005; E-mail: Dwight_Sweigart@brown.edu

Abstract: (η^6 -Naphthalene)Mn(CO)₃⁺ is reduced reversibly by two electrons in CH₂Cl₂ to afford (η^4 -naphthalene)Mn(CO)₃⁻. The chemical and electrochemical reductions of this and analogous complexes containing polycyclic aromatic hydrocarbons (PAH) coordinated to Mn(CO)₃⁺ indicate that the second electron addition is thermodynamically *easier* but kinetically slower than the first addition. Density functional theory calculations suggest that most of the bending or folding of the naphthalene ring that accompanies the $\eta^6 \rightarrow \eta^4$ hapticity change occurs when the second electron is added. As an alternative to further reduction, the 19-electron radicals (η^6 -PAH)Mn(CO)₃ can undergo catalytic CO substitution when phosphite nucleophiles are present. Chemical reduction of (η^6 -naphthalene)Mn(CO)₃⁺ and analogues with *one* equivalent of cobaltocene affords a *syn*-facial bimetallic complex (η^4, η^6 -naphthalene)Mn₂(CO)₅, which contains a Mn–Mn bond. Catalytic oxidative activation under CO *reversibly* converts this complex to the zwitterionic *syn*-facial bimetallic (η^4, η^6 -naphthalene)Mn₂(CO)₆, in which the Mn–Mn bond is cleaved and the naphthalene ring is bent by 45°. Controlled reduction experiments at variable temperatures indicate that the bimetallic (η^4, η^6 -naphthalene)Mn₂(CO)₅ originates from the reaction of (η^4 -naphthalene)Mn(CO)₃⁻ acting as a nucleophile to displace the arene from (η^6 -naphthalene)Mn(CO)₃⁺. Heteronuclear *syn*-facial and *anti*-facial bimetallics are formed by the reduction of mixtures of (η^6 -naphthalene)Mn(CO)₃⁺ and other complexes containing a fused polycyclic ring, e.g., (η^5 -indenyl)Fe(CO)₃⁺ and (η^6 -naphthalene)FeCp⁺. The great ease with which naphthalene-type manganese tricarbonyl complexes undergo an $\eta^6 \rightarrow \eta^4$ hapticity change is the basis for the formation of both the homo- and heteronuclear bimetallics, for the observed two-electron reduction, and for the far greater reactivity of (η^6 -PAH)Mn(CO)₃⁺ complexes in comparison to monocyclic arene analogues.

Introduction

Complexes containing an arene ligand η^6 -bonded to the metal constitute an important class of organometallic compounds. The chemistry exhibited by these complexes often changes dramatically when the arene is switched from monocyclic (e.g., benzene) to polycyclic (e.g., naphthalene). The polycyclic arenes, often termed polycyclic aromatic hydrocarbons or “PAHs”, generally are much more easily displaced from the metal. For example, the complexes (naphthalene)Cr(CO)₃, (naphthalene)RuCp⁺, and (naphthalene)Mn(CO)₃⁺ are all far more reactive than the benzene analogues with respect to substitution of the arene ligand by a variety of nucleophiles, including other arenes.^{1–3} As a consequence, the naphthalene-based systems, in contrast to the benzene-based ones, function

Scheme 1. Reaction of (acenaphthene)Mn(CO)₃⁺ with Nucleophiles



as convenient precursors in a variety of useful synthetic procedures. For example, Scheme 1 illustrates the use of the acenaphthene complex **1** as a manganese-tricarbonyl-transfer

[†] Brown University.

[‡] Providence College.

(1) (a) Kündig, E. P.; Perret, C.; Spichiger, S.; Bernardinelli, G. *J. Organomet. Chem.* **1985**, *286*, 183. (b) Kündig, E. P.; Desobry, V.; Grivet, C.; Rudolph, B.; Spichiger, S. *Organometallics* **1987**, *6*, 1173. (c) Zhang, S.; Shen, J. K.; Basolo, F.; Ju, T. D.; Lang, R. F.; Kiss, G.; Hoff, C. D. *Organometallics* **1994**, *13*, 3692.

(2) (a) McNair, A. M.; Mann, K. R. *Inorg. Chem.* **1986**, *25*, 2519. (b) Bennett, M. A. *Coord. Chem. Rev.* **1997**, *166*, 225.

(3) Sun, S.; Yeung, L. K.; Sweigart, D. A.; Lee, T.-Y.; Lee, S. S.; Chung, Y. K.; Switzer, S. R.; Pike, R. D. *Organometallics* **1995**, *14*, 2613.

(MTT) reagent.³ The $\text{Mn}(\text{CO})_3^+$ moiety is transferred under mild conditions via nucleophilic substitution of the acenaphthene ligand to afford the products indicated. The reaction of **1** with MeCN is complete in less than a minute at room temperature. By way of comparison, the analogous reaction of MeCN with (benzene) $\text{Mn}(\text{CO})_3^+$ has a half-life of about one year. Simply heating **1** with an arene in CH_2Cl_2 provides a convenient general synthesis of (arene) $\text{Mn}(\text{CO})_3^+$. Remarkably, the acenaphthene in **1** can be replaced by the electron-rich complex Cp^*M (M = Fe, Ru, Os) to generate capped metallocene bimetallic species $[\text{MCp}^*\text{Mn}(\text{CO})_3]^+$ (Scheme 1).⁴

The much greater reactivity of polycyclic arene complexes compared to monocyclic analogues is likely due in part to weaker metal–arene bonding in the ground state with the former complexes.⁵ An additional and possibly more significant factor is the facile $\eta^6 \rightarrow \eta^4$ ring slippage that is known to occur with polycyclics and which results in a lowering of the activation energy for nucleophilic attack. Ring slippage is generally believed to be much easier for naphthalene type complexes because the coordinated double bond that is freed upon slippage becomes conjugated with the rest of the hydrocarbon framework, resulting in a more favorable change in aromatic resonance energy than occurs when the coordinated double bond is isolated, as in a monocyclic η^4 -arene complex.³ This behavior is akin to the well-known “indenyl effect”, which refers to the generally much greater reactivity of indenyl complexes compared to cyclopentadienyl analogues.⁶ The $\eta^5 \rightarrow \eta^3$ slippage occurring in indenyl systems has been verified for products resulting from both ligand addition and electron addition to η^5 -indenyl precursors.^{7–10} For example, structural characterization of (η^3 -indenyl) $\text{Fe}(\text{CO})_3^-$ and (η^3 -indenyl)(Cp)Mo[P(OMe)₃]₂ reveals a fold angle between the η^3 carbons and the six-membered indenyl aromatic ring of 22° in both cases.^{9,10} A detailed electrochemical and density functional theory (DFT) study of the reduction of (η^5 -indenyl)(Cp)Mo[P(OMe)₃]₂²⁺ indicated that sequential addition of two electrons occurs fairly rapidly and results in a gradual hapticity change, with the slippage in the singly reduced monocation being almost exactly half that seen in the fully reduced neutral η^3 -indenyl product.⁹ In contrast to this behavior, the complex (η^5 -indenyl) $\text{Fe}(\text{CO})_3^+$ was shown to add a second electron at a much slower rate than the first, suggesting that the slippage is primarily associated with the addition of the second electron.⁷ The radical intermediate (indenyl) $\text{Fe}(\text{CO})_3$ was suggested to be η^5 -bonded, and its CO substitution reactions were shown to be dissociative and much slower than those seen with the (Cp) $\text{Fe}(\text{CO})_3$ radical. This *inverse indenyl effect* for 19-electron radicals has as its origin the same basis as the normal effect seen in 18-electron complexes, i.e., the ability of the indenyl ring system to function as an electron sink (whether or not actual slippage occurs).⁷

It was anticipated⁷ that much of the chemical and electrochemical behavior that differentiates cyclopentadienyl and indenyl ligands would apply as well to benzene and naphthalene ligand comparisons. Several monocyclic arene complexes containing a slipped η^4 -ring have been structurally characterized, e.g., (η^4 -C₆Me₆)Ru(η^6 -C₆Me₆), (η^4 -C₆Me₆)Rh(η^4 -C₆Me₆)⁺, and (η^4 -C₆Me₆)RhCp*.^{11–13} The fold angle in the η^4 -ring in these complexes is 43°, 40°, and 42°, respectively. Detailed electrochemical studies of the precursor complexes (η^6 -C₆Me₆)₂Ru²⁺ and (η^6 -C₆Me₆)MCp*²⁺ (M = Rh, Ir) suggest that overall two-electron reduction follows an EE mechanism, with the interesting feature that the second reduction (E_2°) occurs near to or even positive (anodic) of E_1° .^{11,13–15} The second reduction was found to have a much smaller heterogeneous charge-transfer rate constant (k_s) than the first reduction, which suggests that the first electron addition generates a 19-electron radical, with $\eta^6 \rightarrow \eta^4$ slippage occurring in concert with the addition of the second electron to afford the observed 18-electron product.

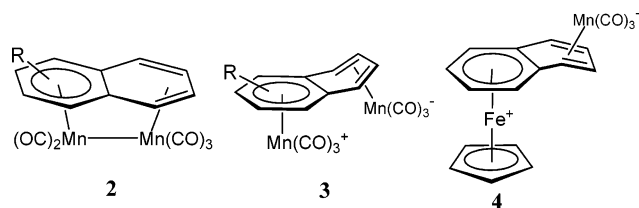
Examples of fully characterized polycyclic arene complexes with slipped η^4 -ligands include the following (the fold angle in the η^4 -ring is given in parentheses): (η^4 -C₁₀H₈)Ru(COD)(PEt₃) (40°),¹⁶ (η^4 -C₁₀Me₈)Ru(η^6 -C₆Me₆) (43°),¹⁷ Co(η^4 -anthracene)₂[–] (28°),¹⁸ (η^4 -naphthalene)Mn(CO)₃[–] (37°),¹⁹ and (η^4 -anthracene)Mn(CO)₃[–] (38°).²⁰ The slipped ring may be generated by ligand addition or electron addition to 18-electron precursors. Thus, reductive electrochemistry would seem to provide an excellent vehicle with which to probe the mechanism and thermodynamics of ring slippage in naphthalene-type complexes, as well as the chemical behavior of the 19-electron organometallic radicals^{21–23} that likely occur as intermediates. In this context, it is perhaps surprising to find that the electrochemical literature dealing with naphthalene-type complexes is quite sparse. Reduction of (η^6 -naphthalene)Cr(CO)₃ is reported²⁴ to occur by a two-electron ECE mechanism to generate (η^4 -naphthalene)Cr(CO)₃^{2–}. A single voltammetric wave was observed, implying that the second reduction is *easier* than the first (E_2° is positive of E_1°). Although slow heterogeneous charge transfer was observed, it was not possible to determine if the slippage occurs with addition of the first or the second electron. Contrasting behavior was found for (η^6 -naphthalene)FeCp⁺, which shows two separate and chemically reversible voltammetric waves separated by ca. 0.6 V.²⁵ In this case ring slippage does not occur, and the reduced product is a formally 20-electron species, in analogy

- (4) Watson, E. J.; Virkaitis, K. L.; Li, H.; Nowak, A. J.; D'Acchioli, J. S.; Yu, K.; Carpenter, G. B.; Chung, Y. K.; Sweigart, D. A. *Chem. Commun.* **2001**, 457.
 (5) Connor, J. A.; Martinho-Simoes, J. A.; Skinner, H. A.; Zafarani-Moattar, M. T. *J. Organomet. Chem.* **1979**, 179, 331.
 (6) Rerek, M. E.; Basolo, F. *J. Am. Chem. Soc.* **1984**, 106, 5908.
 (7) Pevear, K. A.; Banaszak Hall, M. M.; Carpenter, G. B.; Rieger, A. L.; Rieger, P. H.; Sweigart, D. A. *Organometallics* **1995**, 14, 512.
 (8) Lee, S.; Lovelace, S. R.; Cooper, N. J. *Organometallics* **1995**, 14, 1974.
 (9) Stoll, M. E.; Belanzoni, P.; Calhorda, M. J.; Drew, M. G. B.; Félix, V.; Geiger, W. E.; Gamelas, C. A.; Gonçalves, I. S.; Romão, C. C.; Veiros, L. F. *J. Am. Chem. Soc.* **2001**, 123, 10595.
 (10) Forschner, T. C.; Cutler, A. R.; Kullnig, R. K. *Organometallics* **1987**, 6, 889.

- (11) Finke, R. G.; Voegel, R. H.; Laganis, E. D.; Boekelheide, V. *Organometallics* **1983**, 2, 347.
 (12) Thompson, M. R.; Day, C. S.; Day, V. W.; Mink, R. I.; Muetterties, E. L. *J. Am. Chem. Soc.* **1980**, 102, 2979.
 (13) Bowyer, W. J.; Merkert, J. W.; Geiger, W. E.; Rheingold, A. L. *Organometallics* **1989**, 8, 191.
 (14) Pierce, D. T.; Geiger, W. E. *J. Am. Chem. Soc.* **1992**, 114, 6063.
 (15) (a) Bowyer, W. J.; Geiger, W. E. *J. Am. Chem. Soc.* **1985**, 107, 5657. (b) Merkert, J.; Nielson, R. M.; Weaver, M. J.; Geiger, W. E. *J. Am. Chem. Soc.* **1989**, 111, 7084. (c) Nielson, R. M.; Weaver, M. J. *Organometallics* **1989**, 8, 1636.
 (16) Bennett, M. A.; Lu, Z.; Wang, X.; Bown, M.; Hockless, D. C. R. *J. Am. Chem. Soc.* **1998**, 120, 10409.
 (17) Hull, J. W.; Gladfelter, W. L. *Organometallics* **1984**, 3, 605.
 (18) Brennessel, W. W.; Young, V. G.; Ellis, J. E. *Angew. Chem., Int. Ed.* **2002**, 41, 1211.
 (19) Thompson, R. L.; Lee, S.; Rheingold, A. L.; Cooper, N. J. *Organometallics* **1991**, 10, 1657.
 (20) Veauthier, J. M.; Chow, A.; Fraenkel, G.; Geib, S. J.; Cooper, J. N. *Organometallics* **2000**, 19, 661.
 (21) Astruc, D. *Chem. Rev.* **1988**, 88, 1189.
 (22) Geiger, W. E. *Acc. Chem. Res.* **1995**, 28, 351.
 (23) Sun, S.; Sweigart, D. A. *Adv. Organomet. Chem.* **1996**, 40, 171.
 (24) Rieke, R. D.; Henry, W. P.; Arney, J. S. *Inorg. Chem.* **1987**, 26, 420.
 (25) Lacoste, M.; Rabaa, H.; Astruc, D.; Le Beuzec, A.; Saillard, J.-Y.; Precigoux, G.; Courseille, C.; Ardoin, N.; Bowyer, W. *Organometallics* **1989**, 8, 2233.

with certain other first-row transition metal arene complexes, such as $(\eta^6\text{-C}_6\text{Me}_6)\text{CoCp}$ and $(\text{arene})_2\text{Co}^+$.²⁶ Finally, the reduction of $(\eta^6\text{-naphthalene})\text{RuCp}^{*+}$ was reported to occur in two one-electron steps separated by ca. 1.0 V, with the first step chemically reversible and the second irreversible.²⁷

Herein we present a study of the chemical and electrochemical reduction of $(\eta^6\text{-PAH})\text{Mn}(\text{CO})_3^+$ complexes, where PAH represents various substituted naphthalenes, acenaphthene, acenaphthylene, phenanthrene, pyrene, and hexahdopyrene. The mechanistic aspects of $\eta^6 \rightarrow \eta^4$ ring slippage, investigated both experimentally and theoretically, are reported. It is concluded that ring slippage is predominantly associated with electron addition to the 19-electron organometallic radical intermediate $(\eta^6\text{-PAH})\text{Mn}(\text{CO})_3$. Instead of being reduced, and depending on the experimental time scale and the reaction conditions, the $(\eta^6\text{-PAH})\text{Mn}(\text{CO})_3$ intermediate can abstract hydrogen from the reaction medium to give known cyclohexadienyl complexes or undergo electrocatalytic CO substitution by phosphine nucleophiles to afford $(\eta^6\text{-PAH})\text{Mn}(\text{CO})_2\text{PR}_3^+$. In a significant synthetic application, it was found that the fully reduced complex, $(\eta^4\text{-PAH})\text{Mn}(\text{CO})_3^-$, can be used as a nucleophile to displace the PAH from $(\eta^6\text{-PAH})\text{Mn}(\text{CO})_3^+$ and generate homonuclear *syn*-facial η^4, η^6 -bimetallics, such as the generic **2**.²⁸ Complex **2** undergoes reversible electrocatalytic conversion under CO to afford the zwitterionic **3**, which may find application in bimetallic catalysis. In related chemistry, it was found that reduction of $(\eta^6\text{-PAH})\text{Mn}(\text{CO})_3^+$ in the presence of $(\eta^6\text{-naphthalene})\text{ML}^{z+}$ ($\text{ML}^{z+} = \text{FeCp}^+$, $(\text{C}_6\text{Me}_6)\text{Ru}^{2+}$) affords heteronuclear *anti*-facial η^4, η^6 -naphthalene bimetallic complexes such as **4**.



Results and Discussion

Synthesis and Structure of $[(\eta^6\text{-PAH})\text{Mn}(\text{CO})_3]\text{BF}_4$ Complexes. The polycyclic arenes complexed to the manganese tricarbonyl moiety and used in this study are illustrated in Figure 1. These were synthesized by a previously reported procedure, in which $\text{Mn}(\text{CO})_5\text{Br}$ is treated with AgBF_4 in CH_2Cl_2 , the polycyclic arene is then added, and the reaction mixture refluxed.³ With the exception of acenaphthylene (**10**), the product yields were good. Due to the high reactivity of the coordinated naphthalenes, care must be taken to keep the reaction mixture anhydrous and free of any other nucleophilic impurities. This sensitivity to facile nucleophilic attack undoubtedly accounts for the fact that, despite attempts by a number of groups, the parent complex $(\eta^6\text{-naphthalene})\text{Mn}(\text{CO})_3^+$ was not successfully synthesized in significant yield until 1995.³ Although reactive toward nucleophilic solvents, the $[(\eta^6\text{-PAH})\text{Mn}(\text{CO})_3]\text{BF}_4$ complexes are indefinitely stable as solids or in solvents with low donor numbers, such as HPLC-grade CH_2Cl_2 . The high thermal stability coupled with the chemical reactivity of $[(\eta^6\text{-PAH})\text{Mn}(\text{CO})_3]\text{BF}_4$ makes them ideal reagents for the transfer of the $\text{Mn}(\text{CO})_3^+$ moiety to other nucleophilic centers, such as functionalized monocyclic arenes. Due to cost and convenience considerations, the favored MTT reagent is $[(\eta^6\text{-acenaphthene})\text{Mn}(\text{CO})_3]\text{BF}_4$ (Scheme 1).

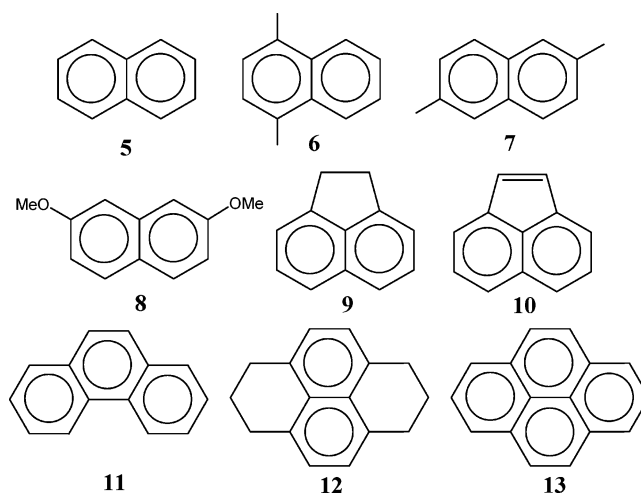


Figure 1. Polycyclic arenes utilized in this study.

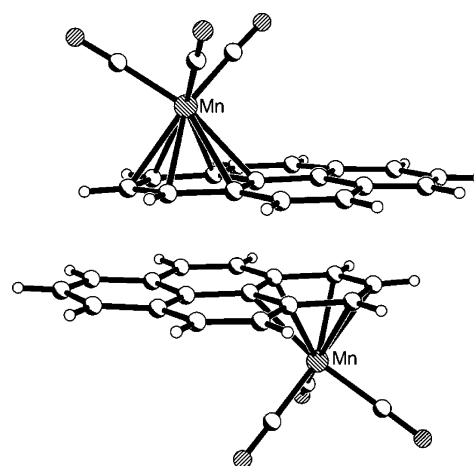


Figure 2. Structure of the cation of $[(\eta^6\text{-pyrene})\text{Mn}(\text{CO})_3]\text{BF}_4$, showing $\pi\text{-}\pi$ stacking.

$\text{Mn}(\text{CO})_3]\text{BF}_4$ complexes are indefinitely stable as solids or in solvents with low donor numbers, such as HPLC-grade CH_2Cl_2 . The high thermal stability coupled with the chemical reactivity of $[(\eta^6\text{-PAH})\text{Mn}(\text{CO})_3]\text{BF}_4$ makes them ideal reagents for the transfer of the $\text{Mn}(\text{CO})_3^+$ moiety to other nucleophilic centers, such as functionalized monocyclic arenes. Due to cost and convenience considerations, the favored MTT reagent is $[(\eta^6\text{-acenaphthene})\text{Mn}(\text{CO})_3]\text{BF}_4$ (Scheme 1).

The X-ray structures of $[(\eta^6\text{-PAH})\text{Mn}(\text{CO})_3]\text{BF}_4$ complexes were determined for PAHs **9**, **10**, and **13**. Crystallographic and structural details may be found as Supporting Information. The most interesting structure of the three is the pyrene (**13**) complex. As shown in Figure 2, the metal coordinates to the aromatic ring with the higher π -bond order, as expected, and as found previously with $\text{Cr}(\text{CO})_3$.²⁹ The pyrene rings engage in $\pi\text{-}\pi$ stacking, with the aromatic rings being parallel and separated by just 3.3 Å (Figure 2). In the case of the manganese tricarbonyl complexes of **9** and **13**, it was found that the $\text{Mn}\text{-C}(\text{arene})$ bond distances for the bridging carbons are ca. 0.07 Å longer than for the unsubstituted ones. It is normal to find greater $\text{Mn}\text{-C}$ bond distances at substituted positions in monocyclic arene complexes.³⁰ In the case of polycyclic arenes, the bond lengthening can be viewed as a predisposition to η^4 -slippage,

(26) Jonas, K.; Deffense, E.; Habermann, D. *Angew. Chem., Int. Ed. Engl.* **1983**, *22*, 716.

(27) (a) Koelle, U.; Wang, M. H. *Organometallics* **1990**, *9*, 195. (b) Gusev, O. V.; Ievlev, M. A.; Peterleitner, M. G.; Peregudova, S. M.; Denisovich, L. I.; Petrovskii, P. V.; Ustynuk, N. A. *J. Organomet. Chem.* **1997**, *534*, 57.

(28) Sun, S.; Dullaghan, C. A.; Carpenter, G. B.; Rieger, A. L.; Rieger, P. H.; Sweigart, D. A. *Angew. Chem., Int. Ed. Engl.* **1995**, *34*, 2540.

(29) Arrais, A.; Diana, E.; Gervasio, G.; Gobetto, R.; Marabello, D.; Stanghellini, P. L. *Eur. J. Inorg. Chem.* **2004**, 1505.

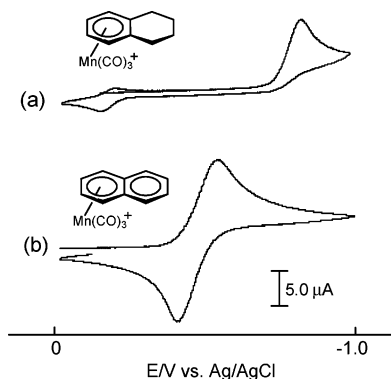
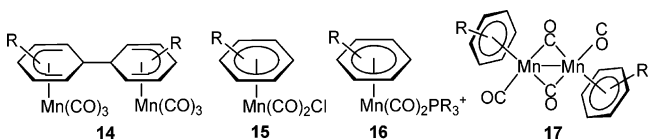


Figure 3. CVs of (a) 1.0 mM [(η^6 -tetralin)Mn(CO) $_3$]PF $_6$ and (b) 1.0 mM [(η^6 -naphthalene)Mn(CO) $_3$]BF $_4$ in CH $_2$ Cl $_2$ /0.10 M Bu $_4$ NPF $_6$ under N $_2$ (g). The working electrode was a 1.0 mm diameter platinum disk, and the scan rate was 0.50 V s $^{-1}$. A ferrocene internal standard had $E_{1/2} = +0.52$ V.

which involves ultimate cleavage of two of the “pre-lengthened” Mn–C bonds. The pre-lengthened bonds and the resonance stabilization of the C=C double bond “freed” upon ring slippage combine to make this a facile process in naphthalene-type systems. In this regard, it is of interest to note that the Mn–C distances for the bridged carbons in the complex with **9** and **13** are ca. 0.05 Å longer than the average Mn–C(arene) bonds found in [(η^6 -C $_6$ Me $_6$)Mn(CO) $_3$][CrI(CO) $_5$].^{30a}

Electrochemical and Chemical Reduction of [(η^6 -PAH)-Mn(CO) $_3$]BF $_4$ Complexes. The reduction chemistry of monocyclic versus polycyclic arene complexes of Mn(CO) $_3^+$ shows fundamental differences that are primarily due to differing propensities for $\eta^6 \rightarrow \eta^4$ ring slippage. Figure 3 shows typical cyclic voltammograms obtained in CH $_2$ Cl $_2$ solvent. The tetralin complex is reduced irreversibly in a one-electron step, while the naphthalene analogue undergoes a chemically reversible overall two-electron reduction to (η^4 -naphthalene)Mn(CO) $_3^-$. We found that tetralin and all other monocyclic arene complexes of Mn(CO) $_3^+$ undergo one-electron irreversible reductions in CH $_2$ Cl $_2$, even at relatively fast scan rates (100 V/s).³¹ The details of this chemistry will be published elsewhere,^{31b} but it may be mentioned that the neutral 19-electron radical obtained from the one-electron chemical or electrochemical reduction of (η^6 -monocyclic arene)Mn(CO) $_3^+$ has been found to give products **14**–**17**, with **14** and **17**³² generally predominating unless a phosphine ligand is present, in which case catalytic substitution to **16** occurs.^{31a} Chemical reduction of (η^6 -benzene)Mn(CO) $_3^+$



at low temperatures with strong reducing agents such as potassium naphthalenide has been shown to afford the slipped

ring complex (η^4 -benzene)Mn(CO) $_3^-$, which undergoes a variety of interesting reactions with electrophilic reagents.³³ It was also shown that (η^4 -benzene)Mn(CO) $_3^-$ reacts with (η^6 -benzene)Mn(CO) $_3^+$ at low temperature to give the cyclohexadienyl coupled product **14** (R = H). In related chemistry, it was reported^{33c} that (η^6 -benzene)Mn(CO) $_3^+$ undergoes a chemically reversible *two-electron* reduction in acetonitrile at a mercury drop electrode (-15 °C and 0.5 V/s scan rate) to give the η^4 -slipped anion. Correspondingly, it was concluded that the reduction potentials for sequential one-electron additions to (η^6 -benzene)Mn(CO) $_3^+$ are in the order $E_2^\circ > E_1^\circ$. We were unable to reproduce the reported electrochemical behavior in acetonitrile solvent and are of the opinion that the suggested potential order $E_2^\circ > E_1^\circ$ may be inaccurate.

The electrochemical data available when this project began clearly established that η^6 -monocyclic arene complexes of Mn(CO) $_3^+$ undergo one-electron reductions in CH $_2$ Cl $_2$ solvent to produce neutral 19-electron radicals that very rapidly couple to form cyclohexadienyl complexes and/or lose CO and then dimerize.³¹ In sharp contrast, the analogous 19-electron radicals obtained from η^6 -polycyclic arene complexes, while being able to dissociate CO or form cyclohexadienyl products under certain conditions, are much more likely to undergo a facile, and in some cases spontaneous, second reduction to afford a stable η^4 -arene product. One of the goals of the present study was to carefully delineate the mechanistic factors responsible for this disparate behavior. To this end, cyclic voltammetry, bulk electrolysis, and chemical reduction techniques were applied over a wide temperature range to manganese complexes with the naphthalene-type arenes listed in Figure 1. The varying observed behaviors, and associated digital simulations, were coupled with high-level DFT calculations to provide a semi-quantitative understanding of $\eta^6 \rightarrow \eta^4$ slippage as it occurs in the electron-transfer and substitution reactions of η^6 -coordinated arenes. The knowledge obtained from these studies has provided an understanding of the reductively activated chemical processes that lead to very interesting new *syn*- and *anti*-facial η^4, η^6 -naphthalene bimetallic complexes such as **2**–**4** (vide infra).

Figures 4 and 5 illustrate typical cyclic voltammograms (CVs) obtained as a function of temperature and scan rate for the manganese complexes of unbridged or “unhindered” naphthalenes **5** and **8** and for the singly bridged acenaphthene (**9**). The doubly bridged hexahydropyrene complex (**12**) gave results very similar to those obtained with **9**. Table 1 summarizes the data for all of the naphthalene-type complexes studied. Inspection of Figures 4 and 5 (which contain ferrocene as an internal potential standard) in conjunction with Figure 3 shows that the complexes of naphthalene and 2,7-dimethoxynaphthalene are reduced in a single voltammetric wave corresponding to two electrons. It is also apparent that the reduction potentials are significantly more positive (by ca. 400 mV) in comparison to that seen with (η^6 -tetralin)Mn(CO) $_3^+$, which undergoes a one-electron irreversible reduction. The CVs of the complexes of **5**

(30) (a) Van Rooyen, P. H.; Geer, L.; Lotz, S. *Acta Crystallogr.* **1990**, C46, 1432. (b) Jeong, E.; Chung, Y. K. *J. Organomet. Chem.* **1992**, 434, 225. (c) Gommans, L. H. P.; Main, L.; Nicholson, B. K. *J. Organomet. Chem.* **1985**, 284, 345. (d) Gagliardini, V.; Balssa, F.; Rose-Munch, F.; Rose, E.; Susanne, C.; Dromzee, Y. *J. Organomet. Chem.* **1996**, 519, 281. (e) Schouteeten, S.; Tranchier, J.-P.; Rose-Munch, F.; Rose, E.; Auffrant, A. *Organometallics* **2004**, 23, 4308. (f) Kang, Y.; Lee, T.; Baik, C.; Lee, S. W.; Kang, S. O.; Shinmyozu, T.; Ko, J. *J. Organomet. Chem.* **2004**, 689, 1586.

(31) (a) Neto, C. C.; Baer, C. D.; Chung, Y. K.; Sweigart, D. A. *Chem. Commun.* **1993**, 816. (b) Reingold, J. A.; Czech, P. T.; Baer, C. D.; Sweigart, D. A., unpublished results.

(32) Morken, A. M.; Eyman, D. P.; Wolff, M. A.; Schauer, S. J. *Organometallics* **1993**, 12, 725.

(33) (a) Thompson, R. L.; Geib, S. J.; Cooper, N. J. *J. Am. Chem. Soc.* **1991**, 113, 8961. (b) Lee, S.; Geib, J.; Cooper, N. J. *J. Am. Chem. Soc.* **1995**, 117, 9572. (c) Lee, S.; Lovelace, S. R.; Arford, D. J.; Geib, S. J.; Weber, S. G.; Cooper, N. J. *J. Am. Chem. Soc.* **1996**, 118, 4190. (d) Shao, L.; Geib, S. J.; Badger, P. D.; Cooper, N. J. *Organometallics* **2003**, 22, 2811. (e) Shao, L.; Geib, S. J.; Cooper, N. J. *Organometallics* **2003**, 22, 4361. (f) Shao, L.; Badger, P. D.; Geib, S. J.; Cooper, N. J. *Organometallics* **2004**, 23, 5939.

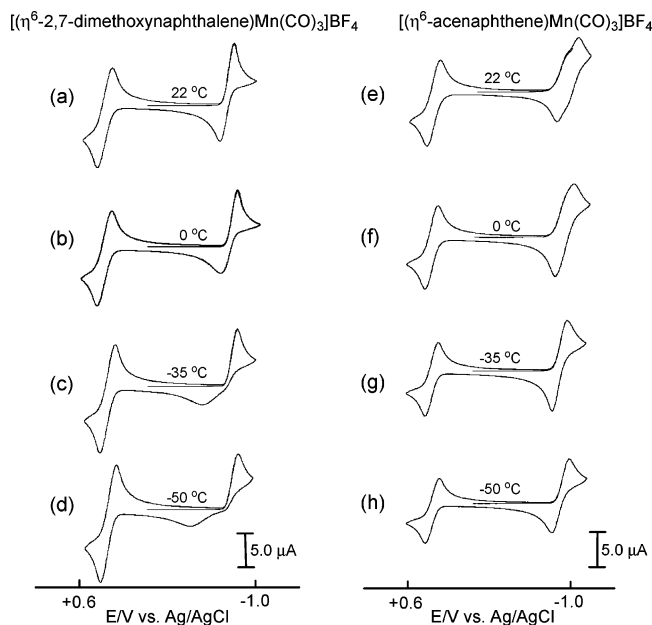


Figure 4. CVs of 1.0 mM $[(\eta^6\text{-}2,7\text{-dimethoxynaphthalene})\text{Mn}(\text{CO})_3]\text{BF}_4$ and 1.0 mM $[(\eta^6\text{-acenaphthene})\text{Mn}(\text{CO})_3]\text{BF}_4$ in $\text{CH}_2\text{Cl}_2/0.10\text{ M Bu}_4\text{NPF}_6$ under $\text{N}_2(\text{g})$. The temperature for each complex is (a,e) 22 °C, (b,f) 0 °C, (c,g) -35 °C, and (d,h) -50 °C. The working electrode was a 1.0 mm diameter glassy carbon disk, and the scan rate was 0.50 V s^{-1} . A ferrocene internal standard had $E_{1/2} = +0.52\text{ V}$.

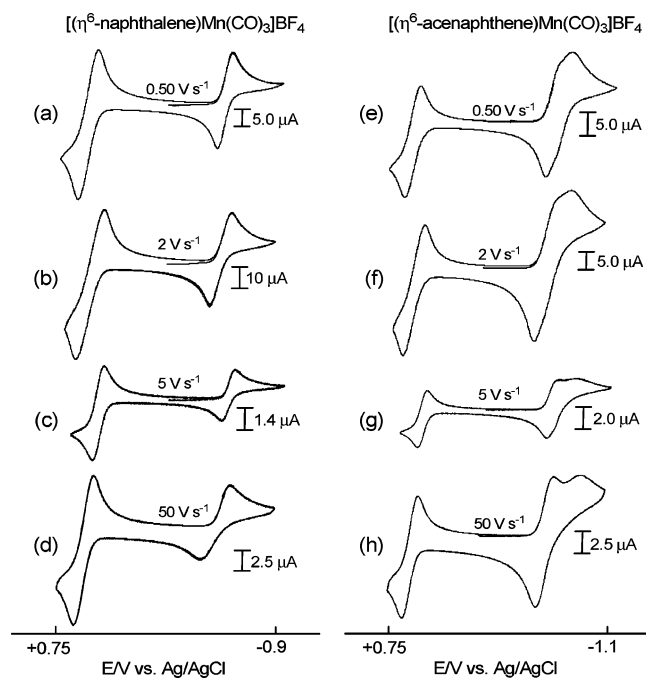


Figure 5. CVs of 1.0 mM $[(\eta^6\text{-naphthalene})\text{Mn}(\text{CO})_3]\text{BF}_4$ and 1.0 mM $[(\eta^6\text{-acenaphthene})\text{Mn}(\text{CO})_3]\text{BF}_4$ in $\text{CH}_2\text{Cl}_2/0.10\text{ M Bu}_4\text{NPF}_6$ under $\text{N}_2(\text{g})$. The scan rate for each complex is (a,e) 0.50 V s^{-1} , (b,f) 2 V s^{-1} , (c,g) 5 V s^{-1} , and (d,h) 50 V s^{-1} . The working electrode for experiments run at 0.50 and 2 V s^{-1} was a 1.0 mm diameter platinum disk for experiments run at 5 and 50 V s^{-1} was a $70\text{ }\mu\text{m}$ platinum disk. All experiments were performed at room temperature. A ferrocene internal standard had $E_{1/2} = +0.52\text{ V}$.

and **8** show obvious signs of slow heterogeneous charge transfer, and the initial interpretation was that reduction to the slipped η^4 -complex occurs via an electrochemical EE mechanism with one or both of the charge transfers being slow.

Table 1. Electrochemical Data for the Reduction of $[(\eta^6\text{-PAH})\text{Mn}(\text{CO})_3]\text{BF}_4$ Complexes in $\text{CH}_2\text{Cl}_2/0.1\text{ M (TBA)PF}_6$ at Room Temperature^a

PAH	observed reduction potential/V
naphthalene (5)	$E_{1/2}(\text{obs})^b = -0.52$
1,4-dimethylnaphthalene (6)	$E_{1/2}(\text{obs})^b = -0.61$
2,6-dimethylnaphthalene (7)	$E_{1/2}(\text{obs})^b = -0.61$
2,7-dimethoxynaphthalene (8)	$E_{1/2}(\text{obs})^b = -0.62$
acenaphthene (9)	$E_{1/2}(1) = -0.62$; $E_{1/2}(2) = -0.72$
acenaphthylene (10)	irreversible; $E_p = -0.33$ at 0.5 V/s
phenanthrene (11)	$E_{1/2}(\text{obs})^b = -0.61$
hexahdropyrene (12)	$E_{1/2}(1) = -0.65$; $E_{1/2}(2) = -0.73$
pyrene (13)	$E_{1/2}(1) = -0.64$; $E_{1/2}(2) \approx -0.74$

^a All potentials were measured versus a Ag/AgCl reference electrode and are adjusted in the table so that the $E_{1/2}$ observed for a ferrocene internal standard is fixed at $+0.50\text{ V}$. ^b $E_{1/2}(\text{obs}) = [E_{1/2}(1) + E_{1/2}(2)]/2$.

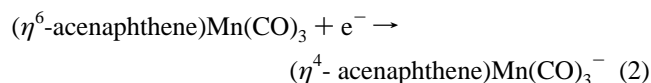
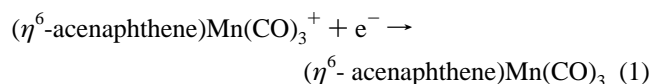
The following analysis, applied to $(\eta^6\text{-naphthalene})\text{Mn}(\text{CO})_3^+$, was found to satisfactorily explain the experimental results for the complexes of all the unbridged naphthalenes **5–8**. The observed EE process occurs as a single wave because $E_{1/2}(2) > E_{1/2}(1)$; furthermore, the observed potential of -0.52 V is well positive of that found^{31b} for $(\eta^6\text{-benzene})\text{Mn}(\text{CO})_3^+$ ($E_p = -0.92\text{ V}$; $E_{1/2} \approx -0.99\text{ V}$), in part because the former potential consists of a composite value equal to $[E_{1/2}(1) + E_{1/2}(2)]/2$.³⁴ By using literature values²⁵ for the *one-electron* reversible reduction potentials of $(\eta^6\text{-arene})\text{FeCp}^+$ to estimate the expected “substituent” effect upon changing from benzene to naphthalene in $(\eta^6\text{-arene})\text{Mn}(\text{CO})_3^+$, it was estimated that $E_{1/2}(1)$ for $(\eta^6\text{-naphthalene})\text{Mn}(\text{CO})_3^+$ would be seen at -0.63 V if the second reduction did not occur spontaneously. Using the observed $E_{1/2}$ of -0.52 V , it was tentatively concluded that $E_{1/2}(1) = -0.63\text{ V}$ and $E_{1/2}(2) = -0.41\text{ V}$ for $(\eta^6\text{-naphthalene})\text{Mn}(\text{CO})_3^+$. With these estimated reduction potentials, digital simulations using DigiSim software³⁵ were performed to mimic the scan rate and temperature behaviors illustrated in Figures 4 and 5. The observed voltammograms were closely reproduced at all scan rates and temperatures as long as the charge-transfer rate constants were kept large for the first reduction and small for the second. In particular, it was concluded that $k_s(1) > 1\text{ cm/s}$, so that nernstian behavior obtains for this step at all available temperatures, with $k_s(2)$ being much smaller and declining to ca. 0.002 cm/s at $-50\text{ }^\circ\text{C}$ (Figure 4).

If the above analysis applied to complexes of unbridged naphthalenes **5–8** is valid, it should provide a basis for understanding the apparently quite different behavior shown in Figures 4 and 5 for the complex with the bridged naphthalene **9** (or double-bridged **12**). The acenaphthene complex shows two closely spaced waves at room temperature: $E_{1/2}(1) = -0.62\text{ V}$; $E_{1/2}(2) = -0.72\text{ V}$. As the scan rate increases, the separation of the two waves was observed to increase, as would be expected for a kinetically shifted wave for $E_p(2)$. Indeed, digital simulations required that $k_s(2)$ be small (ca. 0.02 cm/s) at room temperature in order to reproduce the observed CVs. The temperature dependence of the CVs for $(\eta^6\text{-acenaphthene})\text{Mn}(\text{CO})_3^+$ are especially interesting when compared to the behavior shown by, for example, the 2,7-dimethoxynaphthalene analogue (Figure 4). The CVs for the former complex are remarkable because (1) the two waves evident at room temperature merge

(34) Bard, A. J.; Faulkner, L. R. *Electrochemical Methods*, 2nd ed.; Wiley: New York, 2001.

(35) DigiSim is a registered trademark of Bioanalytical Systems, Inc., West Lafayette, IN.

into one as the temperature is lowered and (2) the wave broadening [$\Delta E_p = E_p(\text{red}) - E_p(\text{ox})$] at low temperature is much less pronounced in comparison to that seen with the complexes of **5–8**. Point (1) means that the wave separation $\Delta E = E_{1/2}(2) - E_{1/2}(1)$, which is ca. -100 mV at room temperature, becomes less negative (or even positive) as the temperature is lowered. The temperature dependence of an electrode potential at constant pressure depends on the entropy according to $(\partial E/\partial T)_p = S/nF$ (where F is the Faraday constant). This expression allows the qualitative temperature dependence of $\Delta E = E_{1/2}(2) - E_{1/2}(1)$ for $(\eta^6\text{-acenaphthene})\text{Mn}(\text{CO})_3^+$ to be understood. The two reductions given in eqs 1 and 2 differ in that ionic charge and hence solvent ordering and/or ion-pairing effects will be prevalent in the reactant for eq 1, but in the product for eq 2. *Relative to the reference electrode potential*, which is the same for both reductions, the prediction based on simple ordering (entropy) considerations is that lowering the temperature will shift $E_{1/2}(1)$ negative and $E_{1/2}(2)$ positive, so that $E_{1/2}(2) - E_{1/2}(1)$ should become more positive as the temperature drops. This is, of course, what is observed. The same behavior likely obtains with the parent $(\eta^6\text{-naphthalene})\text{Mn}(\text{CO})_3^+$ complex also, but this is not easily probed because ΔE for this complex is positive at all temperatures, so that only a single voltammetric wave is observed. It may be noted, however, that ΔE for $(\eta^6\text{-naphthalene})\text{Mn}(\text{CO})_3^+$ can change with temperature by an amount similar (ca. $+100$ mV) to that deduced for $(\eta^6\text{-acenaphthene})\text{Mn}(\text{CO})_3^+$ without affecting the conclusion that $k_s(2)$ is small for this complex.



Point (2) listed above, concerning the lack of pronounced wave broadening (ΔE_p) at low temperature with the complexes of bridged naphthalenes **9** and **12**, is in fact predicted by digital simulations, provided $\Delta E = E_{1/2}(2) - E_{1/2}(1)$ is close to zero at low temperatures. The cathodic shift of $E_p(2)$ at high scan rates at room temperature means $k_s(2)$ must be small, and presumably smaller at low temperatures. This is consistent with observation only if ΔE is near zero. It is concluded that the behavior of complexes with bridged (**9**, **12**) and unbridged (**5–8**) naphthalenes is very similar, both having a slow second electron addition, $k_s(2) \ll k_s(1)$. The primary differences between the two classes of complexes are a more negative ΔE (by several hundred millivolts) and a smaller $k_s(2)$ with the bridged systems. It is tempting to ascribe these differences to a decreased ease of $\eta^6 \rightarrow \eta^4$ slippage caused by the bridging framework connecting the naphthalene subsystem in **9** and **12** (vide infra). The *irreversible* one-electron reduction exhibited by the rigid acenaphthylene complex (**10**, Table 1) would seem to lend support to this hypothesis, although DFT calculations indicate that a meaningful comparison is tenuous in this case because the LUMO in $(\eta^6\text{-acenaphthylene})\text{Mn}(\text{CO})_3^+$ is almost entirely localized on the π -ring, whereas in $(\eta^6\text{-naphthalene})\text{Mn}(\text{CO})_3^+$ it is substantially delocalized on both the metal and the ring

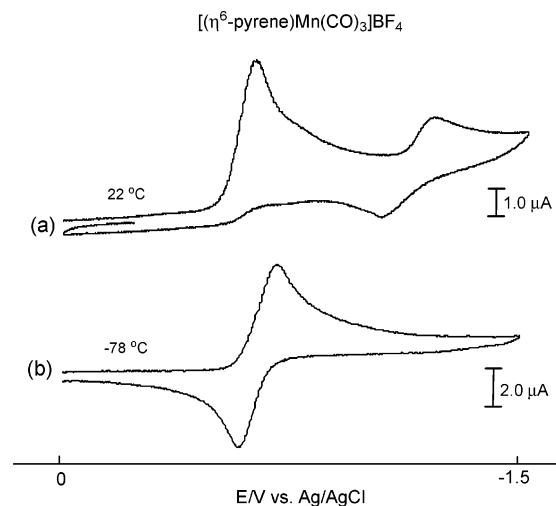


Figure 6. CVs of 1.0 mM $[(\eta^6\text{-pyrene})\text{Mn}(\text{CO})_3]\text{BF}_4$ in $\text{CH}_2\text{Cl}_2/0.10$ M Bu_4NPF_6 under $\text{N}_2(\text{g})$. The temperature was lowered from (a) 20 °C to (b) -78 °C. The working electrode was a 1.0 mm diameter platinum disk, and the scan rate was 0.50 V s^{-1} . A ferrocene internal standard had $E_{1/2} = +0.52$ V.

(vide infra). Consequently, reduction of $(\eta^6\text{-acenaphthylene})\text{Mn}(\text{CO})_3^+$ is best viewed as an essentially ligand-centered process.

The reduction chemistry of the pyrene complex (**13**) proved to be especially interesting. As shown in Figure 6, the CV at room temperature features an irreversible one-electron reduction, followed by a second reversible couple at ca. -1.1 V. Upon lowering the temperature to -78 °C, the second reduction vanishes and the first reduction wave becomes reversible ($E_{1/2} = -0.67$ V). In addition, the current for the low-temperature couple changes to that corresponding to an overall two-electron process. The obvious interpretation is that reduction of $(\eta^6\text{-pyrene})\text{Mn}(\text{CO})_3^+$ at room temperature produces a radical species that reacts rapidly before it can be further reduced to the η^4 -product. The second wave in the room-temperature CV corresponds to reduction of the species formed via a nonredox reaction of the radical, and hence vanishes at low temperature where chemical reversibility obtains. Thus, the behavior of $(\eta^6\text{-pyrene})\text{Mn}(\text{CO})_3^+$ at low temperature is much like that discussed above for the bridged analogues with **9** and **12**. Room-temperature CV results obtained at fast scan rates strongly support this assertion. As shown in Figure 7, the irreversible wave seen at 0.5 V/s becomes partially chemically reversible and splits into two waves as the scan rate increases to 50 V/s. This behavior correlates with that shown in Figure 5g for the complex $(\eta^6\text{-acenaphthene})\text{Mn}(\text{CO})_3^+$.

To better understand the electrochemical results, and most especially to better understand the mechanism of formation of *bimetallic* naphthalene complexes **2** (vide infra), many of the PAH complexes utilized in this study were subjected to bulk electrolysis and bulk chemical reduction. The results of these experiments are discussed with reference to Scheme 2. Bulk electrolysis at room temperature or at -70 °C of the rigid acenaphthylene (**10**) and pyrene (**13**) complexes required only one electron and produced η^5 -cyclohexadienyl complexes **21**, as judged from comparisons of IR spectra with genuine samples of hydride addition products and with published studies of hydride addition to $(\eta^6\text{-PAH})\text{Mn}(\text{CO})_3^+$ complexes.³⁶ Hydrogen abstraction from solvent or adventitious impurities by 19-

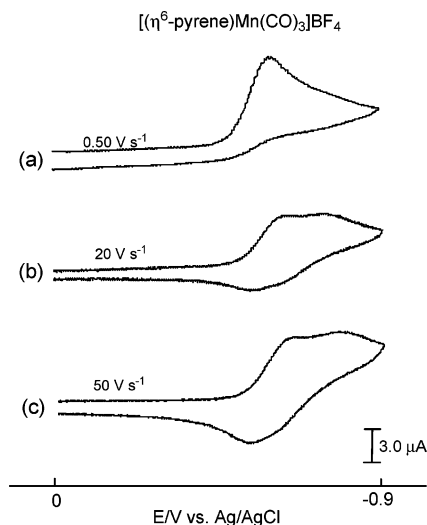


Figure 7. CVs of 1.0 mM $[(\eta^6\text{-pyrene})\text{Mn}(\text{CO})_3]\text{BF}_4$ in $\text{CH}_2\text{Cl}_2/0.10$ M Bu_4NPF_6 under $\text{N}_2(\text{g})$. The temperature was 20°C , and the scan rate was (a) 0.50 V s^{-1} , (b) 20 V s^{-1} , and (c) 50 V s^{-1} . The working electrode was a 1.0 mm diameter platinum disk for (a) and a $70\ \mu\text{m}$ diameter platinum disk for (b,c). A ferrocene internal standard had $E_{1/2} = +0.52\text{ V}$.

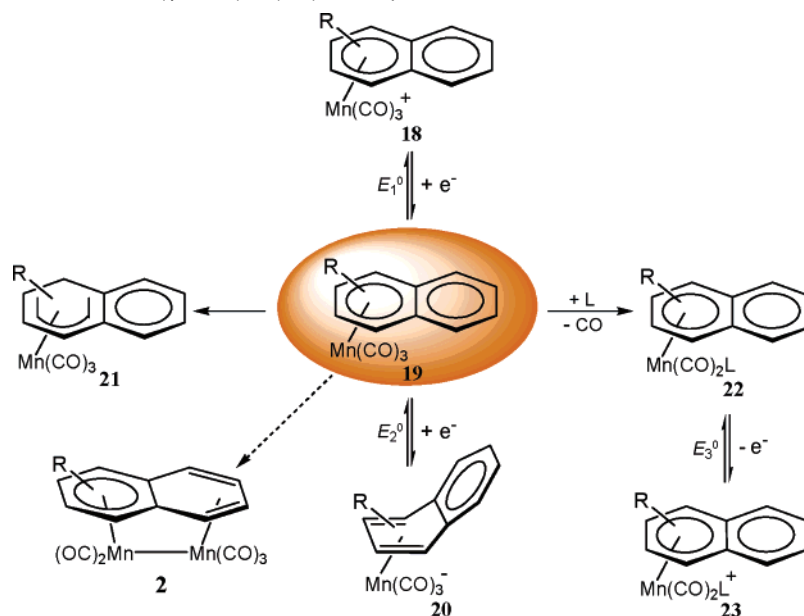
electron η^6 -arene organometallic radicals to afford cyclohexadienyl complexes is well precedented.^{23,27b} The manganese tricarbonyl complexes with naphthalene (**5**) and acenaphthene (**9**) also required one electron for bulk electrolysis at room temperature and similarly produced the η^5 -cyclohexadienyl **21**. However, bulk electrolysis of these two complexes at -70°C consumed two electrons and afforded the η^4 -slipped species **20**, which re-formed the starting material **18** upon subsequent bulk electrochemical oxidation of the reaction mixture at -70°C .

Bulk chemical reductions were performed with cobaltocene in CH_2Cl_2 solvent. Complexes with the unbridged naphthalenes **5**, **6**, and **11** were found to react cleanly with excess Cp_2Co at room temperature to form the slipped η^4 anionic complex **20**. However, the addition of *one* equivalent of Cp_2Co to $(\eta^6\text{-naphthalene})\text{Mn}(\text{CO})_3^+$ or $(\eta^6\text{-1,4-Me}_2\text{naphthalene})\text{Mn}(\text{CO})_3^+$ gave a different product, namely the intriguing bimetallic complex **2**.²⁸ The bridged naphthalene complexes (**9**, **12**) differ

from the unbridged analogues in that excess Cp_2Co at room temperature afforded the bimetallic **2** and not η^4 -**20**. However, the η^4 -**20** anion was produced with excess Cp_2Co at low temperature (-70°C). Room-temperature chemical reduction of the complexes of acenaphthylene (**10**) and pyrene (**13**) was found to give only cyclohexadienyl products. The conclusions from the bulk electrolysis and chemical reduction experiments are in rough agreement with the transient cyclic voltammetric results, in that the η^4 -**20** complex is favored when the time scale is short and/or when the temperature is low. As expected, bridging in the naphthalene ligand seems to hinder (but not eliminate) slippage to the η^4 -complex upon reduction. The interesting question of the mechanism of formation of the bimetallic species **2** is discussed later in this paper.

Cyclic voltammetry of the naphthalene complexes in the presence of the nucleophile $\text{P}(\text{OEt})_3$ gave clear evidence for electrocatalytic CO substitution. This behavior had been reported previously for the monocyclic η^6 -arene complexes of manganese tricarbonyl.^{31a} The propensity for CO substitution in the 19-electron $(\eta^6\text{-naphthalene})\text{Mn}(\text{CO})_3$ radicals follows the qualitative order **11** > **9**, **12** > **5**–**8**. Figure 8 illustrates a typical result obtained with $(\eta^6\text{-phenanthrene})\text{Mn}(\text{CO})_3^+$. On the first cycle in Figure 8b, a new couple appears well negative of the original couple (Figure 8a). The new couple is due to the reduction of $(\eta^6\text{-phenanthrene})\text{Mn}(\text{CO})_2[\text{P}(\text{OEt})_3]^+$, which is formed by CO substitution in **19** to afford the 19-electron radical **22** (Scheme 2). At the potential of its formation, **22** is spontaneously oxidized to **23**, which is then reduced at the second cathodic wave in Figure 8b. On the second CV cycle, the current due to $(\eta^6\text{-phenanthrene})\text{Mn}(\text{CO})_3^+$ has greatly diminished, indicating its depletion at the electrode surface. Concomitant with this current depletion at the first wave, “curve crossing” occurs at the second cathodic wave. The curve crossing and the current depletion at the first cathodic wave are in part due to the cross redox reaction given in eq 3, which has the effect of removing $(\eta^6\text{-phenanthrene})\text{Mn}(\text{CO})_3^+$ from the vicinity of the electrode. The observed potentials indicate that eq 3 is exergonic, and this is the reason for the observed catalysis. Electrocatalytic CO

Scheme 2. Electron-Transfer Reactions of $(\eta^6\text{-PAH})\text{Mn}(\text{CO})_3^+$ Complexes



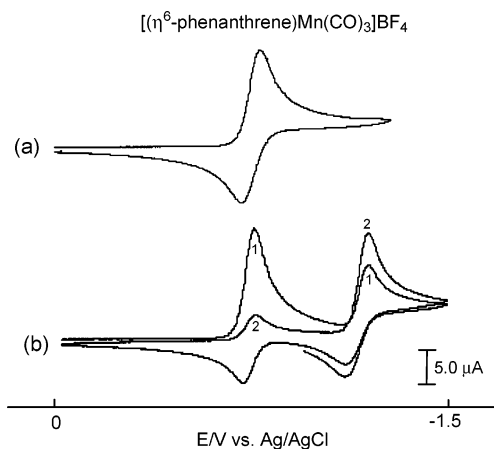
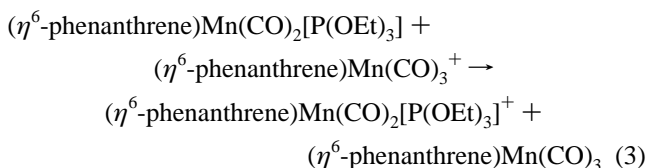


Figure 8. CVs of (a) 1.0 mM $[(\eta^6\text{-phenanthrene})\text{Mn}(\text{CO})_3]\text{BF}_4$ in $\text{CH}_2\text{Cl}_2/0.10\text{ M Bu}_4\text{NPF}_6$ under $\text{N}_2(\text{g})$ and (b) the same with 3.7 mM $\text{P}(\text{OEt})_3$ added. The temperature was $20\text{ }^\circ\text{C}$ and the scan rate 0.50 V s^{-1} . The working electrode was a 1.0 mm diameter glassy carbon disk. A ferrocene internal standard had $E_{1/2} = +0.52\text{ V}$.

substitution in organometallic complexes has been demonstrated for a variety of systems and can be considered a well-established reaction. It is usually initiated by reduction,^{7,23,37} but in rare cases the catalysis can be initiated by oxidation as well.³⁸



Theoretical Calculations of Ring Slippage in $(\eta^6\text{-PAH})\text{Mn}(\text{CO})_3^+$ Complexes. Density functional theory calculations were performed for the cationic, neutral, and anionic members of each of the following manganese complexes: (benzene) $\text{Mn}(\text{CO})_3^z$, (naphthalene) $\text{Mn}(\text{CO})_3^z$, (acenaphthene) $\text{Mn}(\text{CO})_3^z$. All input structures were generated with SPARTAN and minimized with the MFF force field.³⁹ The structures were completely optimized in redundant internal coordinates through DFT calculations as implemented in the NWChem 4.0 package of programs.⁴⁰ The DFT optimizations used Becke's three-parameter functional (B3) along with the Lee–Yang–Parr correlation functional (LYP).⁴¹ All DFT optimizations employed the LANL2DZ basis set with an effective core potential for the Mn atom.⁴²

The results, presented in Table 2, compare favorably with the few available X-ray structures. The atom numbering scheme is given in Figure 9. The calculated Mn–C bond lengths to the η^6 -ring in $(\eta^6\text{-acenaphthene})\text{Mn}(\text{CO})_3^+$ are uniformly about 0.1

Table 2. Results of DFT Calculations for $(\text{arene})\text{Mn}(\text{CO})_3^+$

complex		fold angles ^a	Mn–C _{1,2} ^b	Mn–C _{3,6} ^b	Mn–C _{4,5} ^b
$(\text{benzene})\text{Mn}(\text{CO})_3^z$	cation	0.0, 0.0	2.33	2.33	2.33
	neutral	10.0, 10.1	2.27	2.52	2.94
	anion	39.9, 39.9	2.13	2.24	3.05
$(\text{naphthalene})\text{Mn}(\text{CO})_3^z$	cation	4.6, 4.6	2.29	2.32	2.45
	neutral	16.9, 15.7	2.22	2.40	2.86
	anion	38.6, 38.4	2.13	2.23	3.02
$(\text{acenaphthene})\text{Mn}(\text{CO})_3^z$	cation	4.6, 0.3	2.28	2.34	2.43
	neutral	15.0, 11.0	2.22	2.44	2.86
	anion	35.7, 33.9	2.14	2.27	3.01

^a Listed as dihedral angles (deg) of C1–2–3–4 and C2–1–6–5, respectively. ^b Average of the two bond lengths listed (Å).

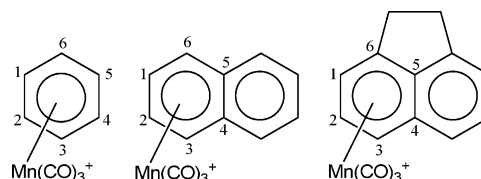


Figure 9. Numbering scheme for DFT calculations.

Å longer than those found experimentally; similarly, the calculated bond lengths in $(\eta^4\text{-naphthalene})\text{Mn}(\text{CO})_3^-$ are uniformly about 0.06 Å longer than those found²⁰ in $(\eta^4\text{-anthracene})\text{Mn}(\text{CO})_3^-$. The fold angle between the diene plane and the rest of the molecule in the η^4 -anions is, of course, one of the key structural features associated with ring slippage. The calculated fold angles, as reflected by the dihedral angles C1–C2–C3–C4 and C2–C1–C6–C5, are calculated to be 38.6° and 38.4° for $(\eta^4\text{-naphthalene})\text{Mn}(\text{CO})_3^-$, which is remarkably close to the value of 37.1° found in the crystal structure.¹⁹ Table 2 shows that the cations with naphthalene and acenaphthene (but not benzene) are calculated to have small nonzero fold angles. The X-ray structure of $(\eta^6\text{-acenaphthene})\text{Mn}(\text{CO})_3^+$ indeed shows corresponding fold angles of 3.5° and 1.3° , with the smaller associated with the C2–C1–C6–C5 angle at the bridging position. Table 2 shows that there is a modest folding upon reduction $z = +1 \rightarrow 0$. However, there is substantially greater folding upon the second reduction $z = 0 \rightarrow -1$. Inspection of the Mn–C bond length changes in Table 2 is revealing. When the first electron adds, the metal “slips” toward C_{1,2}. This results in a modest decrease in Mn–C_{1,2}, a modest increase in Mn–C_{3,6}, and a large increase in Mn–C_{4,5}. When the second electron adds, there is a significant increase in the fold angle by more than 20° from that in the neutral radical. This movement of C4 and C5 away from the metal occurs in concert with movement of C3 and C6 toward the metal, so that the Mn–C_{3,6} bond lengths undergo a substantial decrease while the Mn–C_{4,5} bond lengths increase modestly.

It is concluded that “slipping” of the metal moiety and folding of the ring system are not necessarily synchronous. Significant slipping with lesser folding occurs in the first reduction and vice versa in the second. Since the second reduction is the one with a small heterogeneous rate constant, we propose that folding or bending of the diene plane is a major contributor to the activation energy barrier (as well as the thermodynamics) of reduction. The angles in Table 2 suggest some inhibition of folding at the bridged site in the acenaphthene complex. This unsurprising result may account for the observation that $k_s(2)$ is smaller with the bridged naphthalene complexes. The calculated energies provide insight into the relative ease of

- (36) Sun, S.; Dullaghan, C. A.; Carpenter, G. B.; Sweigart, D. A.; Lee, S. S.; Chung, Y. K. *Inorg. Chim. Acta* **1997**, *262*, 213.
 (37) (a) Bezems, G. J.; Rieger, P. H.; Visco, S. *Chem. Commun.* **1981**, 265. (b) Ruiz, J.; Lacoste, M.; Astruc, D. *J. Am. Chem. Soc.* **1990**, *112*, 5471. (c) Neto, C. C.; Kim, S.; Meng, Q.; Sweigart, D. A.; Chung, Y. K. *J. Am. Chem. Soc.* **1993**, *115*, 2077. (d) Huang, Y.; Neto, C. C.; Pevear, K. A.; Banaszak Holl, M. M.; Sweigart, D. A.; Chung, Y. K. *Inorg. Chim. Acta* **1994**, *226*, 53.
 (38) Zizelman, P. M.; Amatore, C.; Kochi, J. K. *J. Am. Chem. Soc.* **1984**, *106*, 3771.
 (39) Halgren, T. A. *J. Comput. Chem.* **1996**, *17*, 490.
 (40) Harrison, R. J.; et al. *NWChem, A Computational Chemistry Package for Parallel Computers*, Version 4.0; Pacific Northwest National Laboratory: Richland, WA, 2000.
 (41) (a) Becke, A. D. *J. Chem. Phys.* **1993**, *98*, 5648. (b) Lee, C.; Yang, W.; Parr, R. G. *Phys. Rev. B* **1988**, *37*, 785.
 (42) Hay, P. J.; Wadt, W. R. *J. Chem. Phys.* **1985**, *82*, 284.

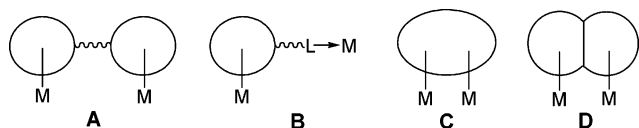


Figure 10. Different types of bimetallic complexes.

slippage/folding in the three ring systems studied (Figure 9). Relative to the energy changes associated with the $z = +1 \rightarrow 0$ and $z = 0 \rightarrow -1$ reductions for (benzene) $\text{Mn}(\text{CO})_3^z$, the energy changes for the naphthalene analogue are -5.1 and -51 kJ, respectively. This means that the relative thermodynamic ease of reduction of naphthalene versus benzene complex is largely associated with the second reduction. We cannot compare the kinetics of reduction of the two systems since the $z = 0 \rightarrow -1$ change for benzene was not observed electrochemically. Possibly the reason it was not observed is very slow kinetics, providing time for the radical neutral species to react by nonredox pathways. With the acenaphthene complex, the energy changes associated with the $z = +1 \rightarrow 0$ and $z = 0 \rightarrow -1$ reductions, relative to those for (naphthalene) $\text{Mn}(\text{CO})_3^z$, were calculated to be $+18$ and $+24$ kJ, respectively. These numbers are in accord with the observation that $\Delta E = E_{1/2(2)} - E_{1/2(1)}$ is considerably more positive for (naphthalene) $\text{Mn}(\text{CO})_3^z$.

Milliken population analyses were performed in order to determine the orbital contributions of the LUMO in (η^6 -arene)- $\text{Mn}(\text{CO})_3^+$ for arene = benzene, naphthalene (**5**), acenaphthene (**9**), and acenaphthylene (**10**). In accordance with calculations reported^{7,25} for (arene) FeCp^+ , $\text{CpFe}(\text{CO})_3^+$, and (indenyl) $\text{Fe}(\text{CO})_3^+$, it was found that the LUMO is more localized on the π -ring in the polycyclic cases. Thus, the LUMO in (η^6 -benzene)- $\text{Mn}(\text{CO})_3^+$ is localized 50% on the metal and 28% on the arene ring. With naphthalene this changes to 30% metal character and 52% ring character, and with acenaphthene (**9**) the LUMO is 40% metal and 43% ring. This shows that the arene ligand in the polycyclic system is better able to function as an “electron sink”, thus facilitating reduction, without, it may be noted, very much folding or bending within the arene ligand in the 19-electron radical. Interestingly, the LUMO in the rigid π -conjugated η^6 -acenaphthylene complex (**10**) is calculated to be 81% localized on the arene ligand and only 12% on the metal. Thus, the radical resulting from one-electron reduction of (η^6 -acenaphthylene) $\text{Mn}(\text{CO})_3^+$ is best described not as a 19-electron organometallic complex but rather as a predominantly 18-electron complex with a ligand-based radical (“ $18 + \delta$ ” complex⁴³).

Bimetallic η^4, η^6 -Naphthalene Complexes. The chemistry described above has been utilized in the synthesis of interesting bimetallic complexes having two metal moieties attached to the same naphthalene ring system, as exemplified by **2–4**. Bimetallic complexes have long attracted attention due to the possibility of realizing useful physical properties stemming from direct or indirect metal–metal interactions.^{28,44–47} The use of such complexes as bimetallic catalysts in which each metal plays an essential cooperative role in the reaction mechanism is especially promising.⁴⁷ Figure 10 shows some classes of bimetallic complexes. In type A, the metals are attached to separate

π -hydrocarbon rings separated by a spacer.⁴⁴ Metal–metal interaction may be possible in this case, depending on the spatial orientations and the nature of the spacer. Type B is a variation on type A, both of which frequently contain a metallocene moiety. In type C bimetallics, the two metals are bonded to the same π -hydrocarbon ring system and may be oriented in a *syn* or *anti* manner.⁴⁵ Bimetallics of type D have the metals bonded *syn* or *anti* to adjacent fused rings.^{44m,46} Most of the reported type D bimetallics contain the indenyl ring system, although ones based on pentalene, azulene, and naphthalene are also known. The few reported^{46d,e} naphthalene bimetallics have the metals situated in an *anti*-facial conformation. In this paper, we report that the polycyclic naphthalene complexes (η^6 -PAH)- $\text{Mn}(\text{CO})_3^+$ form the basis for a quite general synthetic route to *syn*- and *anti*-facial homo- and heteronuclear η^4, η^6 -naphthalene bimetallics, such as **2–4**.⁴⁸ Facile ring slippage and electron transfer in (η^6 -PAH) $\text{Mn}(\text{CO})_3^+$ has been found to play a crucial role in the mechanistic aspects of this chemistry, as is demonstrated below.

As noted above, addition of one equivalent of cobaltocene to (η^6 -PAH) $\text{Mn}(\text{CO})_3^+$ produced the *syn*-facial bimetallic **2** when the PAH was the unbridged naphthalenes **5** and **6**. The complexes with bridged naphthalenes **9** and **12** gave the bimetallic **2**, even when excess cobaltocene was used (at room temperature). The X-ray structures of two of the bimetallics (**24**, **25**) containing 1,4-dimethylnaphthalene (**6**) and hexahydro-pyrene (**12**) are shown in Figure 11. The Mn–Mn bond length is 2.93 and 2.92 Å, respectively, in these complexes. The bond lengths between the metal and the π -ring system clearly demonstrate η^6, η^4 -bonding, as indicated (see Supporting Infor-

(43) (a) Geiger, W. E. *J. Am. Chem. Soc.* **1974**, *96*, 2632. (b) Mao, F.; Philbin, C. E.; Weakley, T. J. R.; Tyler, D. R. *Organometallics* **1990**, *9*, 1510. (c) Mao, F.; Tyler, D. R.; Bruce, M. R. M.; Bruce, A. E.; Rieger, A. L.; Rieger, P. H. *J. Am. Chem. Soc.* **1992**, *114*, 6418. (d) Yang, K.; Bott, S. G.; Richmond, M. G. *Organometallics* **1995**, *14*, 2387.

(44) (a) Koelle, U.; Wang, M. H. *Organometallics* **1990**, *9*, 195. (b) Plitzko, K.-D.; Wehrle, G.; Gollas, B.; Rapko, B.; Dannheim, J.; Boekelheide, V. *J. Am. Chem. Soc.* **1990**, *112*, 6556. (c) Geiger, W. E.; Van Order, N.; Pierce, D. T.; Bitterwolf, T. E.; Rheingold, A. L.; Chasteen, N. D. *Organometallics* **1991**, *10*, 2403. (d) Tilset, M.; Vollhardt, K. P. C.; Boese, R. *Organometallics* **1994**, *13*, 3146. (e) Chin, T. T.; Geiger, W. E. *Organometallics* **1995**, *14*, 1316. (f) Kang, Y. K.; Chung, Y. K.; Lee, S. W. *Organometallics* **1995**, *14*, 4905. (g) Lee, S. S.; Lee, T.-Y.; Lee, J. E.; Lee, I.-S.; Chung, Y. K.; Lah, M. S. *Organometallics* **1996**, *15*, 3664. (h) Bianchini, C.; Meli, A.; Pohl, W.; Vizza, F.; Barbarella, G. *Organometallics* **1997**, *16*, 1517. (i) Heck, J.; Dabek, S.; Meyer-Friedrichsen, T.; Wong, H. *Coord. Chem. Rev.* **1999**, *190*, 1217. (j) Lee, S.-G.; Lee, S. S.; Chung, Y. K. *Inorg. Chim. Acta* **1999**, *286*, 215. (k) Kang, Y. K.; Shin, K. S.; Lee, S.-G.; Lee, I. S.; Chung, Y. K. *Organometallics* **1999**, *18*, 180. (l) Wheatley, N.; Kalck, P. *Chem. Rev.* **1999**, *99*, 3379. (m) Cecon, A.; Santi, S.; Orfan, L.; Bisello, A. *Coord. Chem. Rev.* **2004**, *248*, 683.

(45) (a) Duff, A. W.; Jonas, K.; Goddard, R.; Kraus, H.-J.; Krüger, C. *J. Am. Chem. Soc.* **1983**, *105*, 5479. (b) Ball, R. G.; Edelman, F.; Kiel, G.-Y.; Takats, J. *Organometallics* **1986**, *5*, 829. (c) Astley, S. T.; Takats, J. *J. Organomet. Chem.* **1989**, *363*, 167. (d) Airoidi, M.; Deganello, G.; Gennaro, G.; Moret, M.; Sironi, A. *Organometallics* **1993**, *12*, 3964. (e) Schneider, J. J.; Denninger, U.; Heinemann, C.; Krüger, C. *Angew. Chem., Int. Ed. Engl.* **1995**, *34*, 592. (f) Bögels, G.; Brussaard, H. C.; Hagenau, U.; Heck, J.; Kopf, J.; van der Linden, J. G. M.; Roelofsen, A. *Chem. Eur. J.* **1997**, *3*, 1151.

(46) (a) Churchill, M. R.; Wormald, J. *Inorg. Chem.* **1970**, *9*, 2239. (b) Mues, P.; Benn, R.; Krüger, C.; Tsay, Y.-H.; Vogel, E.; Wilke, G. *Angew. Chem., Int. Ed. Engl.* **1982**, *21*, 868. (c) Jonas, K.; Rüsseler, W.; Krüger, C.; Raabe, E. *Angew. Chem., Int. Ed. Engl.* **1986**, *25*, 928. (d) Rush, B. F.; Lynch, V. M.; Lagowski, J. J. *Organometallics* **1987**, *6*, 1267. (e) Rush, B. F.; Lagowski, J. J. *J. Organomet. Chem.* **1990**, *386*, 37. (f) Jonas, K. *J. Organomet. Chem.* **1990**, *400*, 165. (g) Bonifaci, C.; Cecon, A.; Gambaro, A.; Ganis, P.; Santi, S.; Valle, G.; Venzo, A. *Organometallics* **1993**, *12*, 4211. (h) Winter, R.; Pierce, D. T.; Geiger, W. E.; Lynch, T. J. *Chem. Commun.* **1994**, 1949. (i) Bonifaci, C.; Cecon, A.; Gambaro, A.; Ganis, P.; Santi, S.; Venzo, A. *Organometallics* **1995**, *14*, 2430. (j) Bonifaci, C.; Cecon, A.; Gambaro, A.; Manoli, F.; Mantivani, L.; Ganis, P.; Santi, S.; Venzo, A. *J. Organomet. Chem.* **1998**, *577*, 97. (k) Amatore, C.; Cecon, A.; Santi, S.; Vepeaux, J. N. *Chem. Eur. J.* **1999**, *5*, 3357. (l) Cloke, F. G. N. *Pure Appl. Chem.* **2001**, *73*, 233.

(47) (a) McGovern, P. A.; Vollhardt, K. P. C. *Chem. Commun.* **1996**, 1593. (b) Bosch, B. E.; Brümmer, I.; Kunz, K.; Erker, G.; Fröhlich, R.; Kotila, S. *Organometallics* **2000**, *19*, 1255. (c) Guo, N.; Li, L.; Marks, T. J. *J. Am. Chem. Soc.* **2004**, *126*, 6542. (d) Comte, V.; Le Gendre, P.; Richard, P.; Moïse, C. *Organometallics* **2005**, *24*, 1439.

(48) A preliminary report of some aspects of this chemistry is given in ref 28.

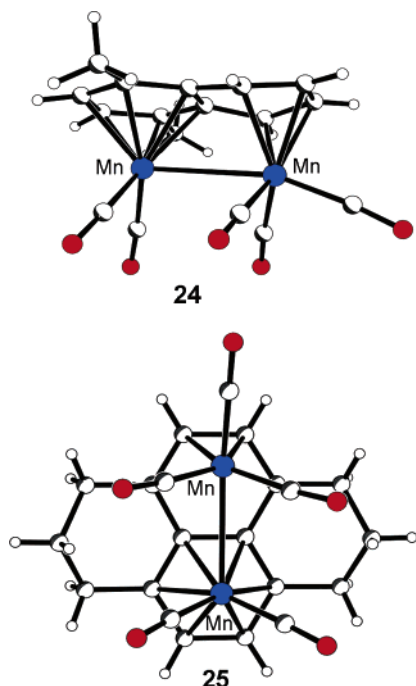
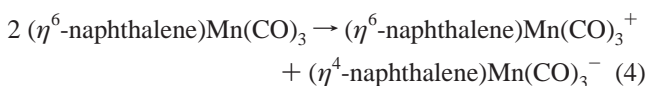


Figure 11. X-ray structures of bimetallic complexes (η^4,η^6 -1,4-Me₂-naphthalene)Mn₂(CO)₅ (**24**) and (η^4,η^6 -hexahydropyrene)Mn₂(CO)₅ (**25**).

mation). The Mn–C bond lengths involving the inner η^4 -diene carbons are about 0.06 Å longer in **25** than in **24**, which is the only significant difference in the metal–arene bond distances in the two structures.

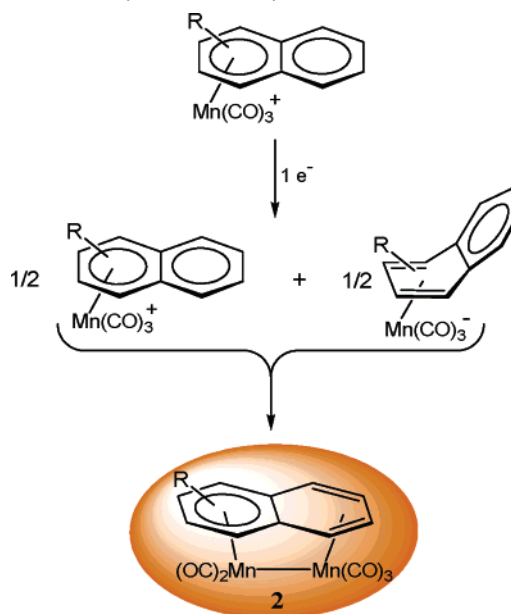
To probe the mechanism of formation of these unusual products, a variety of variable-temperature bulk electrolysis and chemical reduction experiments were performed. Bulk electrolysis of (η^6 -naphthalene)Mn(CO)₃⁺ in CH₂Cl₂ at –60 °C, stopped after the addition of *one* equivalent of electrons, was shown by IR spectra to give a clean 1:1 mixture of η^6 -cation and η^4 -anion at this temperature. This confirms that the disproportionation reaction in eq 4 is thermodynamically favored, as implied by the voltammetric results discussed above. Warming the mixture of η^6 -cation and η^4 -anion led to



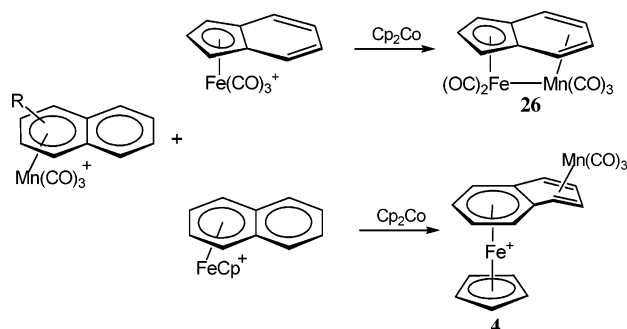
no change in the IR spectrum until ca. 0 °C, at which temperature reaction occurred to afford the bimetallic **2**. Significantly, one-electron bulk electrolysis at –70 °C of the complex with the bridged acenaphthene (**9**) also gave a mixture of η^6 -cation and η^4 -anion that converted to the corresponding bimetallic **2** upon warming to room temperature. Related experiments using cobaltocene were done with (η^6 -1,4-Me₂-naphthalene)Mn(CO)₃⁺. One equivalent of Cp₂Co added to the η^6 -cation at –80 °C afforded a 1:1 mixture of η^6 -cation and η^4 -anion, which again converted to the bimetallic (**24**) upon warming to –5 °C. In agreement with this result, the addition of (η^6 -1,4-Me₂-naphthalene)Mn(CO)₃⁺ to the corresponding η^4 -anion, prepared by room-temperature reduction of the η^6 -cation with two equivalents of cobaltocene, similarly produced **24**.

The obvious conclusion from these experiments is that the η^4 -anion acts as a nucleophile to displace the PAH ligand from the η^6 -cation, as shown in Scheme 3. Crucial to this mechanism

Scheme 3. Electron-Transfer-Induced Formation of η^4,η^6 -Bimetallic Naphthalene Complexes



Scheme 4. Electron-Transfer-Induced Formation of *Syn*- and *Anti*-Facial Heterobimetallic Complexes



is the coexistence of the η^6 -cation and η^4 -anion, a condition that is fulfilled because E_2° is close to or positive of E_1° for (η^6 -PAH)Mn(CO)₃⁺ complexes (vide supra). Additionally, the mechanism requires that the naphthalene ligand in the η^6 -cation be labile; as shown above, this condition is certainly met. In contrast to this type of behavior, (η^6 -benzene)Mn(CO)₃⁺ and (η^4 -benzene)Mn(CO)₃[–] are reported^{33a,c} to react at low temperatures via ring coupling to yield the dimeric η^5 -cyclohexadienyl complex [(η^5 -C₆H₆)Mn(CO)₃]₂.

In chemistry perhaps analogous to that shown in Scheme 3, it was found that cobaltocene addition to a 1:1 mixture of (η^6 -naphthalene)Mn(CO)₃⁺ and (η^5 -indenyl)Fe(CO)₃⁺ led to the *syn*-facial heteronuclear bimetallic **26** according to Scheme 4.²⁸ It is likely that the mechanism involves reduction of the indenyl complex, which then attacks and displaces the naphthalene ligand from the η^6 -manganese cation. In this case, as in the reactions giving homonuclear manganese bimetallics, CO loss from one of the metals allows the formation of a metal–metal bond. When there is no CO (or other ligand) available to dissociate, the formation of a metal–metal bonded *syn*-facial bimetallic is prevented by the 18-electron rule. For example, reduction of a mixture of (η^6 -naphthalene)FeCp⁺ and (η^6 -PAH)Mn(CO)₃⁺ by cobaltocene affords the zwitterionic *anti*-facial bimetallic **4**. By variation of the R group in Scheme 4, it was established that the naphthalene ring in **4** originates with the

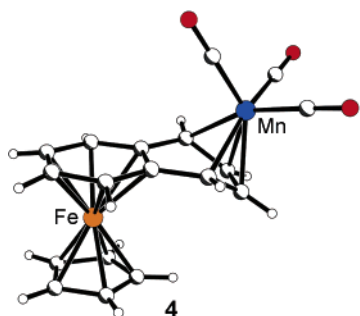
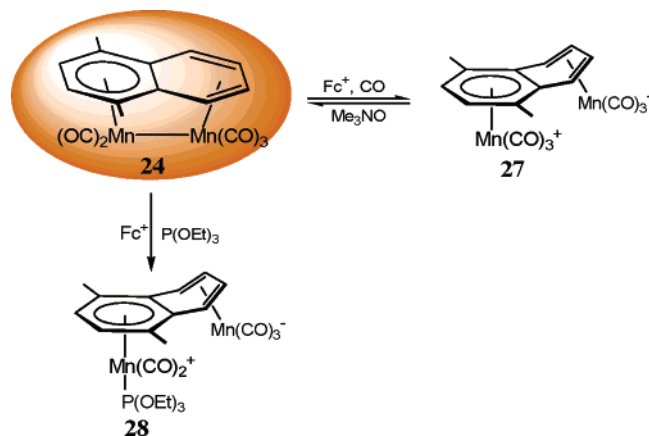


Figure 12. X-ray structure of the zwitterionic bimetallic **4**.

Scheme 5. Formation of Zwitterionic *Syn*-Facial Bimetallic Complexes



iron and not the manganese. The X-ray structure of **4** is given in Figure 12. The bend in the diene portion of the naphthalene ligand in **4** is 35°.

It was found that a zwitterionic bimetallic of the *syn*-facial variety could be obtained from bimetallic **24** by the chemistry illustrated in Scheme 5. Complex **24** is relatively stable under an atmosphere of CO at room temperature, but upon addition of a few mole percent of the oxidant ferrocenium ion, a rapid conversion to the fascinating zwitterionic **27** occurs. The ferrocenium serves to initiate an electrocatalytic process in which **24** is oxidized and reacts to give **27**⁺, which then undergoes electron exchange with **24** to propagate the process. The initial “kick start” by ferrocenium is needed to weaken the Mn–Mn bond so that CO addition can occur and the Mn–Mn bond can be cleaved. Reaction of **24** in the presence of P(OEt)₃ instead of CO produced the analogous substituted zwitterionic **28**. Of course, to cleave the Mn–Mn bond in **24** upon ligand addition, as required by the 18-electron rule, it is necessary for the naphthalene ring in **27** and **28** to undergo bending or folding. The X-ray structures of both **27** and **28** were determined and are given in Figure 13. The fold angle of the diene plane from the rest of the naphthalene ring system is 45° in both complexes.

The transformation **24** + CO → **27** is especially remarkable because it was found to be reversible. Thus, the addition of Me₃NO to **27** led to rapid conversion back to **24** (with liberation of CO₂). The neutral but highly polar **27** presents interesting possibilities for bimetallic catalysis because the metals are in close proximity, oppositely charged, and able to convert reversibly to the nonpolar Mn–Mn bonded **24**. Obviously, zwitterionic *anti*-facial bimetallics such as **4** do not offer these features. IR spectroscopy indicates that the separation of charges in zwitterion **27** is substantial, albeit incomplete. The IR

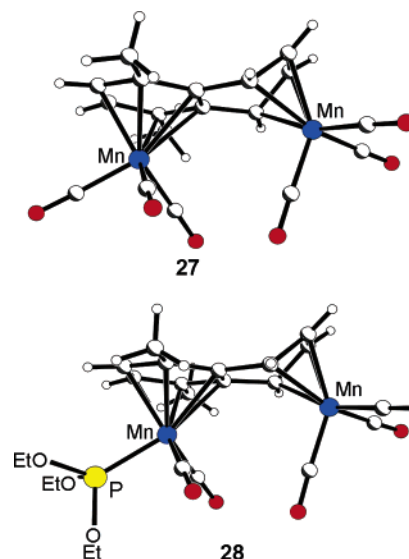


Figure 13. X-ray structures of zwitterionic *syn*-facial bimetallics **27** and **28**.

spectrum of **27** in the ν_{CO} region contains bands at 2050 and 1980(br) cm⁻¹ for the η^6 -bonded Mn(CO)₃⁺ fragment and at 1980(br) and 1880 cm⁻¹ for the η^4 -bonded Mn(CO)₃⁻ fragment. By comparison, the ν_{CO} bands for (η^6 -1,4-Me₂naphthalene)Mn(CO)₃⁺ and for (η^4 -1,4-Me₂naphthalene)Mn(CO)₃⁻ occur at 2072, 2014 cm⁻¹ and 1937, 1842 cm⁻¹, respectively.

Cyclic voltammetry of bimetallic **24** under N₂ in CH₂Cl₂ at 0 °C shows a chemically reversible one-electron oxidation at a potential near that of ferrocene ($E_{1/2} = +0.45$ V relative to Fc⁺/Fc = +0.50 V). Under CO the oxidation is irreversible as catalytic waves appear. Comparison of the CV of **24** to that of zwitterion **27** shows that the electrochemical behavior of the former under CO is the same as that of the latter under N₂, indicating that the two species are intimately coupled via electron transfer.⁴⁹

Conclusions

The chemistry of (η^6 -arene)Mn(CO)₃⁺ is very dependent on the nature of the arene. Monocyclic arenes such as benzene are relatively inert to nucleophilic displacement, whereas naphthalene-type polycyclic aromatic arenes (PAHs) are rapidly displaced from the metal; as a consequence, (η^6 -PAH)Mn(CO)₃⁺ complexes serve as excellent manganese-tricarbonyl-transfer reagents. The basis for this reactivity difference is a facile $\eta^6 \rightarrow \eta^4$ hapticity change that occurs with the naphthalene-type complexes in the presence of nucleophiles. Correspondingly, the two classes of arene complexes also behave very differently when chemically or electrochemically reduced. Thus, (η^6 -benzene)Mn(CO)₃⁺ undergoes a chemically irreversible one-electron reduction at room temperature in CH₂Cl₂, whereas (η^6 -naphthalene)Mn(CO)₃⁺ is reduced reversibly by two electrons to afford (η^4 -naphthalene)Mn(CO)₃⁻. Electrochemical measurements indicate that the second electron addition is easier (less negative potential) than the first, such that $\Delta E = E_{1/2}(2) - E_{1/2}(1)$ is positive by about 200 mV at room temperature. The rate of charge transfer is much slower for the second electron addition than it is for the first [$k_s(2) < k_s(1)$]. DFT calculations suggest that most of the bending or folding of the naphthalene

(49) Reingold, J. A.; Sweigart, D. A., research in progress.

ring that accompanies the $\eta^6 \rightarrow \eta^4$ hapticity change occurs when the second electron is added, thus accounting for the slow charge transfer observed for this step. With “bridged” naphthalenes such as acenaphthene and hexahydropyrene, $\Delta E = E_{1/2}(2) - E_{1/2}(1)$ is slightly negative (by ca. -100 mV) at room temperature and $k_s(2)$ is further decreased, suggesting, as might be expected, that the bridge hinders to some extent both the kinetics and thermodynamics of the folding process. As an alternative to undergoing spontaneous or nearly spontaneous reduction to $(\eta^4\text{-PAH})\text{Mn}(\text{CO})_3^-$, the 19-electron radicals $(\eta^6\text{-PAH})\text{Mn}(\text{CO})_3$ can undergo catalytic CO substitution when phosphite nucleophiles are present.

Chemical reduction of $(\eta^6\text{-naphthalene})\text{Mn}(\text{CO})_3^+$ (or related manganese PAH complexes) with *one* equivalent of cobaltocene affords a unique *syn*-facial bimetallic complex $(\eta^4, \eta^6\text{-naphthalene})\text{Mn}_2(\text{CO})_5$, which contains a Mn–Mn bond. Catalytic oxidative activation under CO *reversibly* converts this complex to the zwitterionic *syn*-facial bimetallic $(\eta^4, \eta^6\text{-naphthalene})\text{Mn}_2(\text{CO})_6$, in which the Mn–Mn bond is cleaved and the naphthalene ring is bent by 45° . The facile reversible cleavage of the Mn–Mn bond to give a zwitterionic product suggests that this chemistry and synthetic methodology may find useful applications in bimetallic catalysis. Controlled reduction experiments as a function of temperature strongly indicate that the bimetallic $(\eta^4, \eta^6\text{-naphthalene})\text{Mn}_2(\text{CO})_5$ originates from the reaction of $(\eta^4\text{-naphthalene})\text{Mn}(\text{CO})_3^-$, acting as a nucleophile to displace the arene from $(\eta^6\text{-naphthalene})\text{Mn}(\text{CO})_3^+$. Heteronuclear *syn*-facial and *anti*-facial bimetallics can be obtained by the reduction of mixtures of $(\eta^6\text{-naphthalene})\text{Mn}(\text{CO})_3^+$ and other complexes containing a fused polycyclic ring, e.g., $(\eta^5\text{-indenyl})\text{Fe}(\text{CO})_3^+$ and $(\eta^6\text{-naphthalene})\text{FeCp}^+$. The basis for the formation of both the homo- and heteronuclear bimetallics is the great ease with which the ring in $(\eta^6\text{-PAH})\text{Mn}(\text{CO})_3^+$ slips and can be subsequently displaced by organometallic nucleophiles.

Experimental Section

Complexes **1**, **2**, **25**, and **26** were prepared by literature methods, as were the $(\eta^6\text{-polycyclic arene})\text{Mn}(\text{CO})_3\text{BF}_4$ complexes containing the naphthalenes **5–13**.^{3,28} All solvents were purchased from commercial sources as ACS grade or better and used without further purification. HPLC-grade methylene chloride (Fisher Scientific Co.) was stored and opened under nitrogen. Cobaltocene (Strem Chemical Co.) was stored at low temperature under argon and generally used within two weeks of purchase. Cobaltocene solutions were prepared and used under an atmosphere of nitrogen. Elemental analyses were performed by Quantitative Technologies Inc.

$(\eta^4, \eta^6\text{-Naphthalene})\text{Mn}(\text{CO})_3\text{FeCp}$ (4**)**. Cp₂Co (0.4 mmol), $(\eta^6\text{-naphthalene})\text{Mn}(\text{CO})_3\text{BF}_4$ (0.2 mmol), $(\eta^6\text{-naphthalene})\text{FeCp}]\text{PF}_6$ (0.2 mmol), and 10 mL of CH₂Cl₂ were mixed under N₂. After being stirred for 4 h at room temperature, the mixture was chromatographed quickly through a short column of deactivated neutral alumina (10% H₂O), using hexane eluant to remove nonpolar impurities and dichloromethane eluant to obtain the product. The solvent was then removed and the dark solid washed with pentane to afford the product in 38% yield. Anal. Calcd for C₁₈H₁₃O₃FeMn: C, 55.67; H, 3.35. Found: C, 55.82; H, 3.23. Selected IR (CH₂Cl₂, cm⁻¹): 1969, 1881, 1865. ¹H NMR (CD₂-Cl₂, 300 MHz, room temperature, δ ppm): 6.05–6.15 (m, 2H), 5.46–5.52 (m, 2H), 4.82–4.89 (m, 2H), 4.47 (s, Cp), 2.29–2.35 (m, 2H). A dark red-brown crystal of **4** suitable for X-ray analysis was grown via pentane diffusion into a diethyl ether solution under N₂ at -20°C .

$(\eta^4, \eta^6\text{-1,4-Me}_2\text{naphthalene})\text{Mn}_2(\text{CO})_5$ (24**)**. Cp₂Co (0.2 mmol), $(\eta^6\text{-1,4-Me}_2\text{naphthalene})\text{Mn}(\text{CO})_3\text{BF}_4$ (0.2 mmol), and 10 mL of CH₂-Cl₂ were mixed under N₂, stirred at room temperature for 15 min, and

then chromatographed quickly through a short column of deactivated neutral alumina (10% H₂O) with CH₂Cl₂ as eluant. The solvent was removed and the dark solid washed with pentane to give product in 55% yield. Anal. Calcd for C₁₇H₁₂O₃Mn₂: C, 49.77; H, 2.68. Found: C, 50.25; H, 2.96. Selected IR (CH₂Cl₂, cm⁻¹): 2004, 1941, 1885. ¹H NMR (CD₂Cl₂, 300 MHz, room temperature, δ ppm): 5.40–5.47 (m, 2H), 5.20 (s, 2H), 4.02–4.10 (m, 2H), 1.77 (s, Me). A crystal of **24** suitable for X-ray analysis was grown via pentane diffusion into a CH₂-Cl₂ solution under N₂ at -20°C .

$(\eta^4, \eta^6\text{-1,4-Me}_2\text{naphthalene})\text{Mn}_2(\text{CO})_6$ (27**)**. Complex **24** (0.05 mmol) was dissolved in CH₂Cl₂ (3 mL). Carbon monoxide was bubbled through the solution, and ferrocenium hexafluorophosphate (0.1 equiv) was added. After 10 min, the IR spectrum verified that the starting complex had disappeared. The solution was then concentrated and chromatographed through deactivated neutral alumina (10% H₂O) with CH₂Cl₂ as eluant. The solvent was removed and the residue washed with pentane to afford an orange-brown powder in 91% yield. Anal. Calcd for C₁₈H₁₂O₆Mn₂: C, 49.80; H, 2.79. Found: C, 49.91; H, 2.70. Selected IR (CH₂Cl₂, cm⁻¹): 2050, 1989, 1979, 1880. ¹H NMR (CD₂Cl₂, 300 MHz, room temperature, δ ppm): 5.85–5.95 (m, 2H), 5.02 (s, 2H), 2.65–2.75 (m, 2H), 2.12 (s, 2Me). Orange-brown crystals suitable for X-ray analysis were grown via pentane diffusion into a diethyl ether solution under N₂ at -20°C .

$(\eta^4, \eta^6\text{-1,4-Me}_2\text{naphthalene})\text{Mn}_2(\text{CO})_5\text{P}(\text{OEt})_3$ (28**)**. Complex **24** (0.05 mmol), P(OEt)₃ (0.1 mmol), and CH₂Cl₂ (3 mL) were combined under nitrogen, and ferrocenium hexafluorophosphate (0.01 mmol) was added to the solution. After 20 min, the solution was concentrated and chromatographed through deactivated neutral alumina (10% H₂O) with CH₂Cl₂ as eluant. The solvent was removed, and the residue was washed with pentane to give an orange-brown powder in 79% yield. Anal. Calcd for C₂₃H₂₇O₈PMn₂: C, 48.27; H, 4.76. Found: C, 47.98; H, 4.79. Selected IR (CH₂Cl₂, cm⁻¹): 1991, 1962, 1937, 1877, 1859. ¹H NMR (CD₂Cl₂, 300 MHz, room temperature, δ ppm): 5.70–5.76 (m, 2H), 4.74 (d, 2H), 3.85–4.00 (m, OCH₂), 2.70–2.75 (m, 2H), 2.07 (s, 2Me), 1.25–1.40 (m, 3Me). Orange crystals suitable for X-ray analysis were grown via pentane diffusion into a CH₂Cl₂ solution under N₂ at -20°C .

Electrochemistry. Voltammetric experiments were done under a blanket of nitrogen that was saturated with solvent. The electrolyte was 0.10 M Bu₄NPF₆, which was synthesized by the metathesis of Bu₄NBr and HPF₆, recrystallized from hot ethanol, and dried under vacuum. The solvent used was HPLC-grade CH₂Cl₂ (Fisher Scientific catalog no. D143-1). The solvent was found to be entirely suitable for use without additional “purification”. Voltammetry at low temperatures utilized a simple slush bath, with a thermocouple probe inserted to monitor the temperature.⁵⁰ Cyclic voltammetry was done with EG&G 173/175/179 potentiostatic instrumentation. A standard three-electrode system was used. The working electrode was a 1 mm diameter platinum or glassy carbon disk, and the counter electrode was a platinum wire. The reference was a Metrohm Ag/AgCl electrode filled with CH₂Cl₂/0.10 M Bu₄NClO₄ and saturated with LiCl. The reference electrode was separated from the test solution by a salt bridge containing 0.10 M Bu₄NPF₆ in the solvent in use. Ferrocene was generally added as an internal potential standard. Bulk electrolyses were done with a platinum-basket working electrode and a platinum-mesh counter electrode, which was separated from the test solution by a salt bridge. IR spectra of solutions undergoing electrolysis or chemical reduction were recorded at variable temperatures via a Remspec fiber optic probe. Digital simulation of proposed mechanisms utilized the program DigiSim.³⁵

Theoretical Calculations. Density functional theory calculations were performed for the cationic, neutral, and anionic members of each of the following manganese complexes: (benzene)Mn(CO)₃²⁺, (naphthalene)Mn(CO)₃²⁺, and (acenaphthene)Mn(CO)₃²⁺. All input structures were generated with SPARTAN and minimized with the MFF force field.

(50) Stone, N. J.; Sweigart, D. A.; Bond, A. M. *Organometallics* **1986**, *5*, 2553.

The structures were completely optimized in redundant internal coordinates through DFT calculations as implemented in the NWChem 4.0 package of programs. The DFT optimizations used Becke's three-parameter functional (B3) along with the Lee–Yang–Parr correlation functional (LYP). All DFT optimizations employed the LANL2DZ basis set with an effective core potential for the Mn atom.

Crystallography. X-ray data collection was carried out using a Bruker single-crystal diffractometer equipped with an APEX CCD area detector and controlled by SMART version 5.0. Collection was done at either room temperature or 100 K. Data reduction was performed by SAINT version 6.0, and absorption corrections were applied by SADABS version 2.0. The structures were typically determined by direct methods and refined on F^2 by use of programs in SHELXTL version 5.0. Most hydrogen atoms appeared in a difference map, or they were generally inserted in ideal positions, riding on the atoms to which they are attached.

Acknowledgment. We are grateful to the donors of the Petroleum Research Fund, administered by the American Chemical Society, and to the National Science Foundation

(CHE-0308640) for support of this research. Additionally, it is a pleasure to acknowledge stimulating discussions with Jason D'Acchioli of The Ohio State University.

Supporting Information Available: Crystallographic data including positional parameters, thermal parameters, bond distances, and bond angles (CIF) are included for $[(\eta^6\text{-acenaphthylene})\text{Mn}(\text{CO})_3]\text{BF}_4$, $[(\eta^6\text{-pyrene})\text{Mn}(\text{CO})_3]\text{BF}_4$, $[(\eta^6\text{-acenaphthene})\text{Mn}(\text{CO})_3]\text{BF}_4$, $[(\eta^6\text{-hexahdropyrene})\text{Mn}(\text{CO})_3]\text{BF}_4$, $(\eta^4, \eta^6\text{-1,4-Me}_2\text{naphthalene})\text{Mn}_2(\text{CO})_5$, $(\eta^4, \eta^6\text{-naphthalene})\text{Mn}(\text{CO})_3\text{FeCp}$, $(\eta^4, \eta^6\text{-1,4-Me}_2\text{naphthalene})\text{Mn}_2(\text{CO})_6$, and $(\eta^4, \eta^6\text{-1,4-Me}_2\text{naphthalene})\text{Mn}_2(\text{CO})_5\text{P}(\text{OEt})_3$. [These files have also been deposited with the Cambridge Crystallographic Data Center as registry numbers CCDC-266764 through CCDC 266771, respectively.] Complete ref 40 available (PDF). This material is available free of charge via the Internet at <http://pubs.acs.org>.

JA0527370